Chapter 7
Coupled Oscillators

This chapter deals with finite amplitude vibrations of coupled oscillators having two or more degrees of freedom. As a rule, the governing equations are not integrable and can be solved only by numerical integration. The numerical solutions have to be visualized by the Poincaré map. For mechanical systems with weak coupling the variational-asymptotic method is applicable. This enables one to study, among others, the bifurcation of nonlinear normal modes, KAM-theory for coupled conservative oscillators, and synchronization of the coupled self-excited oscillators.

7.1 Conservative Oscillators

Differential Equations of Motion. To begin with, let us consider some simple nonlinear coupled conservative oscillators.

EXAMPLE 7.1. Nonlinear mass-spring oscillators. Two equal masses m move horizontally under the action of three springs with cubic nonlinearity (see Fig. 7.1). Derive the equations of motion for these oscillators.

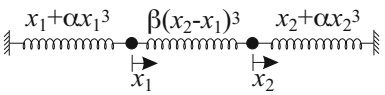

Fig. 7.1 Coupled oscillators with nonlinear springs

Let x_1 and x_2 be the displacements from the equilibrium positions of the point-masses and let $x = (x_1, x_2)$. The kinetic energy of the masses is given by

$$K(\dot{x}) = \frac{1}{2} m(\dot{x}_1^2 + \dot{x}_2^2).$$

We assume that all springs are nonlinear, but the connecting spring differs from the anchor springs. We write the potential energy of the springs in the form

$$U(x)=\frac{1}{2}k[x_1^2+\frac{\alpha}{2l_0^2}x_1^4+x_2^2+\frac{\alpha}{2l_0^2}x_2^4+\frac{\beta}{2l_0^2}(x_2-x_1)^4].$$

Thus, Lagrange's equations are

$$m\ddot{x}_1+kx_1+k\frac{\alpha}{l_0^2}x_1^3-k\frac{\beta}{l_0^2}(x_2-x_1)^3=0,$$
$$m\ddot{x}_2+kx_2+k\frac{\alpha}{l_0^2}x_2^3+k\frac{\beta}{l_0^2}(x_2-x_1)^3=0.$$

Dividing these equations by kl_0 and introducing the dimensionless quantities

$$\bar{t}=\omega_0 t,\quad \bar{x}_i=\frac{x_i}{l_0},\quad i=1,2,$$

where $\omega_0=\sqrt{k/m}$, we rewrite them as (the bar is dropped)

$$\begin{aligned}\ddot{x}_1+x_1+\alpha x_1^3-\beta(x_2-x_1)^3=0,\\ \ddot{x}_2+x_2+\alpha x_2^3+\beta(x_2-x_1)^3=0.\end{aligned}\tag{7.1}$$

EXAMPLE 7.2. A spring pendulum. A point mass m is attached to a linear spring of stiffness k that is swinging in the vertical plane as shown in Fig. 7.2. Derive the equations of motion for this pendulum.

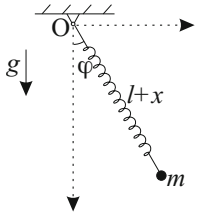

Fig. 7.2 Spring pendulum

Denoting the elongation of the spring from the equilibrium length l by x, we write the kinetic and potential energies of the pendulum as

$$K(q,\dot{q})=\frac{1}{2}m[\dot{x}^2+(l+x)^2\dot{\varphi}^2],$$
$$U(q)=\frac{1}{2}kx^2+mg(l+x)(1-\cos\varphi)-mgx,$$

where $q=(x,\varphi)$. Lagrange's equations read

$$m\ddot{x}+kx-m(l+x)\dot{\varphi}^2-mg\cos\varphi=0,$$
$$m(l+x)^2\ddot{\varphi}+mg(l+x)\sin\varphi+2m(l+x)\dot{x}\dot{\varphi}=0.$$

Dividing the first equation by m and the second one by $m(l+x)^2$, we obtain

$$\ddot{x}+\omega_2^2x-(l+x)\dot{\varphi}^2-g\cos\varphi=0,$$
$$\ddot{\varphi}+\frac{g\sin\varphi+2\dot{x}\dot{\varphi}}{l+x}=0,$$

where $\omega_2^2=k/m$.

Note that the linearization of the above equations leads to uncoupled equations describing two independent modes of vibrations: a spring mode with a frequency

ω_2 and a pendulum mode with a frequency $\omega_1 = \sqrt{g/l}$. However, when $\omega_2 \approx 2\omega_1$ the two modes are coupled causing the energy transfer between them.

EXAMPLE 7.3. Chain of nonlinear mass-spring oscillators. A chain of points of equal mass m connected by identical nonlinear springs is constrained to move in the longitudinal direction (see Fig. 7.3). Derive the equation of motion.

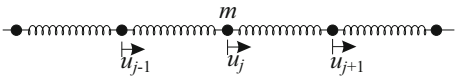

Fig. 7.3 Chain of nonlinear mass-spring oscillators

Denoting the displacement of the point-mass j from the equilibrium position by $u_j(t)$ we write down the kinetic energy of the chain

$$K(\dot{u}) = \frac{1}{2} m \sum_j \dot{u}_j^2.$$

The potential energy of the chain is the sum of energies of the springs. Considering the springs with cubic nonlinearity, we take the potential energy in the form

$$U(u) = \frac{1}{2} k \sum_j [(u_j - u_{j-1})^2 + \frac{\alpha}{2l_0^2}(u_j - u_{j-1})^4],$$

where l_0 is the original length of the spring which is equal to the spacing between the point-masses in equilibrium. Here we assume that the ends of the chain are fixed: $u_0 = u_{n+1} = 0$. So, the chain has n degrees of freedom. Lagrange's equations of this chain read

$$m\ddot{u}_j + k[(u_j - u_{j-1}) + \frac{\alpha}{l_0^2}(u_j - u_{j-1})^3] - k[(u_{j+1} - u_j) + \frac{\alpha}{l_0^2}(u_{j+1} - u_j)^3] = 0$$

for all $j = 1, \ldots, n$. Introducing the dimensionless quantities

$$\bar{t} = \omega_0 t, \quad \bar{u}_j = \frac{u_j}{l_0},$$

where $\omega_0 = \sqrt{k/m}$, we rewrite these equations in the form (the bar is dropped)

$$\ddot{u}_j + (u_j - u_{j-1}) + \alpha(u_j - u_{j-1})^3 - (u_{j+1} - u_j) - \alpha(u_{j+1} - u_j)^3 = 0.$$

Hamilton's Equations. The equations of motion derived in the previous paragraph are differential equations of second order. As a rule they are not integrable and can be solved only by numerical integration. For this purpose it is more convenient to

transform them from Lagrange's to the equivalent Hamilton's form.[1] This transformation is quite straightforward. Let us do it in the most general case.

We take the differential of the Lagrange function as function of the generalized coordinates $q = (q_1, \ldots, q_n)$ and velocities $\dot{q} = (\dot{q}_1, \ldots, \dot{q}_n)$

$$dL = \sum_{j=1}^{n} \left(\frac{\partial L}{\partial q_j} dq_j + \frac{\partial L}{\partial \dot{q}_j} d\dot{q}_j \right).$$

We introduce the generalized impulses as $p = (p_1, \ldots, p_n)$, where $p_j = \partial L / \partial \dot{q}_j$. Then Lagrange's equations becomes

$$\dot{p}_j = \frac{\partial L}{\partial q_j}.$$

Thus, the above differential can be written as

$$dL = \sum_{j=1}^{n} (\dot{p}_j dq_j + p_j d\dot{q}_j).$$

Since the second term in the summand is equal to $p_j d\dot{q}_j = d(p_j \dot{q}_j) - \dot{q}_j dp_j$, we present this equation in the form

$$d\left(\sum_{j=1}^{n} p_j \dot{q}_j - L \right) = \sum_{j=1}^{n} (-\dot{p}_j dq_j + \dot{q}_j dp_j). \tag{7.2}$$

The expression in parentheses on the left-hand side represents energy of the system; cf. (2.28). Expressing it in terms of the coordinates and impulses means doing Legendre's transform [5] of $L(q, \dot{q})$ with respect to $\dot{q}$. We call the result Hamilton function

$$H(q, p) = \sum_{j=1}^{n} p_j \dot{q}_j - L.$$

Equation (7.2) then implies

$$\dot{q}_j = \frac{\partial H}{\partial p_j}, \quad \dot{p}_j = -\frac{\partial H}{\partial q_j}, \tag{7.3}$$

for all $j = 1, 2, \ldots, n$. These are the equations of motion in Hamilton's (or canonical) form. For any conservative mechanical system with n degrees of freedom this system of $2n$ differential equations of first order replaces n differential equations of second order. If the Hamilton function does not depend explicitly on time, then

[1] Except the convenience for numerical integration Hamilton's form of equations of motion provides a number of advantages just as the representation of motion as a phase curve in the phase space, the treatment of various theoretical questions of mechanics as well as the links to physics and thermodynamics [5].

$$\frac{d}{dt}H = \sum_{j=1}^{n}\left(\frac{\partial H}{\partial q_j}\dot{q}_j + \frac{\partial H}{\partial p_j}\dot{p}_j\right) = 0,$$

so the conservation of the energy $H(q,p) = E_0$ follows.

For the coupled oscillators in example 7.1 the dimensionless Hamilton's function reads

$$H(q,p) = \frac{1}{2}(p_1^2 + p_2^2) + \frac{1}{2}[q_1^2 + \frac{\alpha}{2}q_1^4 + q_2^2 + \frac{\alpha}{2}q_2^4 + \frac{\beta}{2}(q_2 - q_1)^4], \tag{7.4}$$

where $x_1 = q_1$ and $x_2 = q_2$. Hamilton's equations become

$$\begin{aligned} \dot{q}_1 &= p_1, \quad \dot{p}_1 = -q_1 - \alpha q_1^3 + \beta(q_2 - q_1)^3, \\ \dot{q}_2 &= p_2, \quad \dot{p}_2 = -q_2 - \alpha q_2^3 - \beta(q_2 - q_1)^3. \end{aligned} \tag{7.5}$$

Phase Curves and Poincaré Map. Just as for single oscillators, the solutions of Hamilton's equations (7.3) for coupled oscillators may be drawn as phase curves in the $2n$-dimensional (q,p)-phase space. There is only one phase curve passing through a given point of the phase space. Therefore, one may think of points in the phase space as particles of some fluid which move in accordance with Hamilton's equations. This motion generates a flow with an interesting property that it conserves volumes of the phase space (Liouville's theorem). This means that if we draw all phase curves that begin from points inside a region of volume V in the phase space at time $t = 0$, then the end points of these phase curves at time t fill a region with the same volume. Indeed, the velocity of this Hamilton's flow, $(\dot{q}, \dot{p})$, is divergent-free

$$\operatorname{div}(\dot{q}, \dot{p}) = \sum_{j=1}^{n}\left(\frac{\partial \dot{q}_j}{\partial q_j} + \frac{\partial \dot{p}_j}{\partial p_j}\right) = \sum_{j=1}^{n}\left(\frac{\partial^2 H}{\partial p_j \partial q_j} - \frac{\partial^2 H}{\partial q_j \partial p_j}\right) = 0,$$

which implies Liouville's theorem.

To see what the phase curves look like let us turn to example 7.1. Equations (7.5) do not permit in general analytical solutions except perhaps, the case $\beta = 0$ for which the oscillators become uncoupled. We analyze first this simple case. Since now the oscillators are uncoupled, the energy of each of them is conserved

$$\frac{1}{2}p_j^2 + \frac{1}{2}q_j^2 + \frac{\alpha}{4}q_j^4 = E_{j0}, \quad j = 1,2.$$

This leads immediately to the solution in form of elliptic integrals obtained already in Section 5.1

$$t = t_0 \pm \int_{q_{j0}}^{q_j} \frac{dx}{\sqrt{2E_{j0} - x^2 - \frac{\alpha}{2}x^4}}.$$

Based on this solution we may express q_j and p_j as periodic functions of t with two different periods

$$T_j = 2\int_{q_{jm}}^{q_{jM}} \frac{dx}{\sqrt{2E_{j0} - x^2 - \frac{\alpha}{2}x^4}}.$$

Note that the periods T_j as well as the corresponding frequencies $\omega_j = 2\pi/T_j$ depend on the initial energies of the oscillators. It turns out that for integrable systems there exist always angle-action variables (φ, I), with $\varphi = (\varphi_1, \ldots, \varphi_n)$ and $I = (I_1, \ldots, I_n)$, in terms of which the Hamilton function becomes independent of φ: $H = H(I)$ (see [5]). The solution of Hamilton's equations

$$\dot{\varphi}_j = \frac{\partial H}{\partial I_j} = \omega_j(I_j), \quad \dot{I}_j = -\frac{\partial H}{\partial \varphi_j} = 0$$

is quite simple in these variables: $\varphi_j = \omega_j t + \varphi_{j0}$ and $I_j = \text{const}$. For our uncoupled oscillators the action variables I_j are computed as follows

$$I_j = \frac{1}{2\pi}\oint p_j dq_j,$$

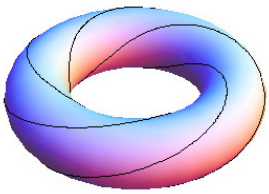

Fig. 7.4 A phase curve on torus

while the angle variables φ_j correspond to the angular times. Topologically, each phase curve can then be regarded as a curve on a 2-D torus shown in Fig. 7.4. If the frequency ratio ω_2/ω_1 is a rational number, then the phase curves are closed orbits on the torus corresponding to the periodic motions. If this ratio is irrational, the phase curves wind around endlessly on the torus and correspond to the quasiperiodic motions (cf. the Lissajous figures in exercise 2.5). The tori are called invariant because each phase curve starting on some torus stays there forever. By changing the energy of one of the oscillators, we get the one-parameter family of invariant tori which fill the whole three-dimensional energy level surface.

As soon as $\beta \neq 0$ we expect that Hamilton's equations of these coupled oscillators become non-integrable. KAM theory which will be considered in Section 7.3 predicts that for sufficiently small β most of invariant tori, corresponding to irrational frequency ratios and called non-resonant tori, survive this small disturbance: they are just slightly deformed. The resonant tori and maybe some of the non-resonant tori are destroyed by the disturbance, resulting in layers of chaotic motion and filling the space between preserved tori. However, the volume of the chaotic motion and destroyed tori tends to zero as $\beta \to 0$ (see Section 7.3).

Thus, from what is said above it is clear that, for $\beta \neq 0$, the only way to obtain the solution is to do numerical integration. Assume that we have found by numerical integration a particular solution of (7.5) satisfying the initial conditions $q(0) = q_0$ and $p(0) = p_0$. Then the question arises: how can we visualize the phase curve in the four-dimensional phase space? One circumstance makes this visualization easier: due to the energy conservation the phase curve must lie on the 3-D energy level surface

$$H(q_1, q_2, p_1, p_2) = E_0, \tag{7.6}$$

with E_0 being the initial energy. However, it is still difficult for us to draw a curve on a 3-D energy level surface given *implicitly* in this form. A great help came from Poincaré, who introduced a fixed 2-D cut plane traverse to the flow. If we plot the intersection of the phase curve with this plane, the generated map, called Poincaré map, (cf. Fig. 6.8), enables one to follow the traces of the phase curve on this plane.

The Poincaré map can be constructed numerically as follows. First, we use the energy conservation to find the initial velocity $p_1(0)$ from the randomly chosen initial data for q_1, q_2, p_2. Next, the numerical integration generates trajectories lying on the three-dimensional energy level surface. Finally, we pick out points of intersection of trajectories crossing the cut plane $q_1 = 0$ with the positive velocity $p_1 > 0$. In this case the Poincaré section is defined by

$$\Sigma = \{q_1 = 0, p_1 > 0\}.$$

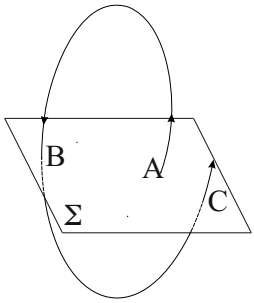

Fig. 7.5 Poincaré map

Note that an additional restriction on the sign of the velocities at the intersecting points is posed. The reason is that we want the Poincaré map to be orientation preserving [20]. In Fig. 7.5 this is realized by counting only points A and C, but not point B where the trajectory crosses the cut plane with a negative velocity.

Imposing condition (7.6) and $q_1 = 0$ for the specific Hamilton's function (7.4) we obtain

$$p_1 = \pm\sqrt{2E_0 - \frac{1}{2}(\alpha+\beta)q_2^4 - q_2^2 - p_2^2}.$$

Together with (7.6) this defines the Poincaré map for the coupled mass-spring nonlinear oscillators. The points of the Poincaré map fill the interior of a region with the boundary corresponding to the condition $p_1 = 0$

$$2E_0 = \frac{1}{2}(\alpha+\beta)q_2^4 + q_2^2 + p_2^2.$$

Numerical Simulations. Numerical simulations of the Poincaré maps require a little bit more elaborated commands in *Mathematica* than those used in previous Chapters to simulate the phase curves in the 2-D phase plane. We took here the code originally written by E. Weisstein[2] and slightly modified it to adapt to our particular problem.

The Poincaré maps of the dynamical system (7.5) are shown in Fig. 7.6 for the fixed energy level $E_0 = 0.4$ and for $\alpha = 1$ in two cases: a) $\beta = 0.1$ (left), and b) $\beta = 0.4$ (right). Looking at these Poincaré maps we can recognize the qualitatively

[2] This open source code, together with some explanations, can be found on the website `http://mathworld.wolfram.com/notebooks/DynamicalSystems/SurfaceofSection.nb`

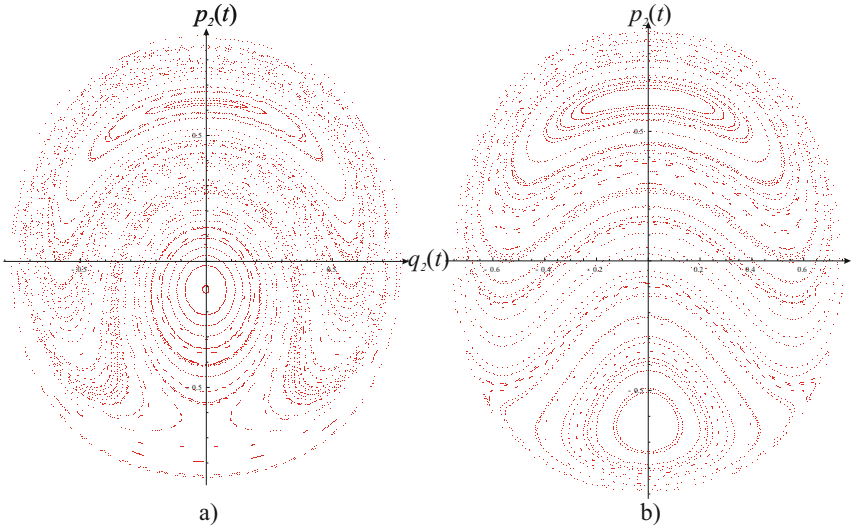

Fig. 7.6 Poincaré maps for $E_0 = 0.4$ and $\alpha = 1$: a) $\beta = 0.1$, b) $\beta = 0.4$

different behavior in case a) and b). In case b) there are two fixed points corresponding to the periodic solutions[3] with $q_2 = q_1$ and $q_2 = -q_1$. Such special periodic solutions are called nonlinear normal modes. Both symmetric ($q_2 = q_1$) and antisymmetric normal modes ($q_2 = -q_1$) are orbitally stable as they are surrounded by points of intersections of trajectories on non-resonant invariant tori with the Poincaré section. It turns out that the bifurcation occurs for $\beta < 1/4$. For these values of β the antisymmetric mode becomes unstable, whereas the two bifurcating modes are orbitally stable. Note the closed loop starting and ending at the unstable saddle point and resembling the separatrix in 2-D case (in fact, there are two such loops, but the second one is difficult to observe as it is very near to the boundary curve of the plot). This path is called a "homoclinic orbit" [49] and is formed by trajectories that approach the saddle point after an infinite number of positive and negative iterations. The homoclinic orbits are recognized as a mechanism for generation of chaotic motions in weakly coupled oscillators.

It is interesting to note that this type of bifurcation for nonlinear coupled oscillators is sensitive only to the ratio $\beta/\alpha = \kappa$, called a coupling factor, as shown in Fig. 7.7. In this case $\alpha = 0.1$ while $\beta = 0.01$ and 0.04 so that the coupling factor remains the same as in the previous simulations. In the next Section we will use this fact to provide the asymptotic analysis of the variational problem containing the small parameters α and β.

[3] The proof of existence of at least n periodic solutions passing through each stable equilibrium state for conservative mechanical system having n degrees of freedom at any fixed level of energy can be found in [34, 52].

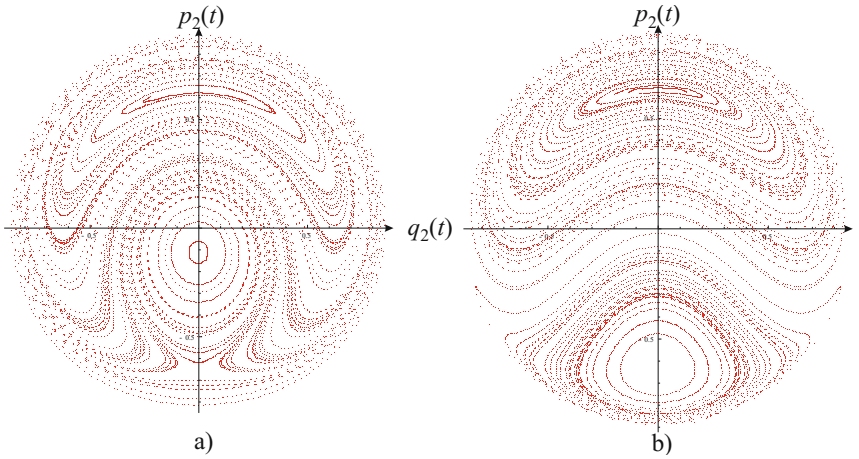

Fig. 7.7 Poincaré maps for $E_0 = 0.4$ and $\alpha = 0.1$: a) $\beta = 0.01$, b) $\beta = 0.04$

7.2 Bifurcation of Nonlinear Normal Modes

This Section analyzes the bifurcation of nonlinear normal modes observed by numerical integration in the previous Section with the help of the variational-asymptotic method.

Nonlinear Normal Modes and the Modal Equation. Let us turn back to Lagrange's equations (7.1) for the nonlinear coupled oscillators and rewrite them in the form

$$\ddot{x} = -\frac{\partial U}{\partial x}, \quad \ddot{y} = -\frac{\partial U}{\partial y}, \tag{7.7}$$

where $x = x_1$, $y = x_2$, and $U(x,y)$ is the potential energy. As we know, the energy of this system is conserved

$$\frac{1}{2}(\dot{x}^2 + \dot{y}^2) + U(x,y) = E_0.$$

We seek the nonlinear normal modes as periodic solutions by assuming y as a function of x, without direct reference to time t, and try to eliminate t in these equations. Using the chain rule

$$\dot{y} = y'\dot{x}, \quad \ddot{y} = y''\dot{x}^2 + y'\ddot{x},$$

with prime denoting the derivative of y with respect to x, and substituting this into the second of (7.7) to get

$$-\frac{\partial U}{\partial y} = y''\dot{x}^2 - y'\frac{\partial U}{\partial x}. \tag{7.8}$$

Next, we substitute $\dot{y}$ into the energy conservation

$$\frac{1}{2}\dot{x}^2(1+y'^2)+U(x,y)=E_0.$$

Solving this equation with respect to $\dot{x}$ and substituting into (7.8), we obtain finally

$$2(E_0-U)y''+(1+y'^2)(\frac{\partial U}{\partial y}-y'\frac{\partial U}{\partial x})=0. \tag{7.9}$$

This is the differential equation to determine the nonlinear normal modes, called a modal equation.

The system of coupled oscillators in example 7.1, due to its symmetry, admits quite simple nonlinear normal modes for which $y=cx$. Such normal modes are called similar normal modes. Indeed, substituting this form of solution into (7.9) and keeping in mind that

$$U(x,y)=\frac{1}{2}[x^2+\frac{\alpha}{2}x^4+y^2+\frac{\alpha}{2}y^4+\frac{\beta}{2}(y-x)^4],$$

we obtain

$$\frac{\partial U}{\partial y}-y'\frac{\partial U}{\partial x}=cx+\alpha c^3x^3+\beta(c-1)^3x^3-c[x+\alpha x^3-\beta x^3(c-1)^3]=0.$$

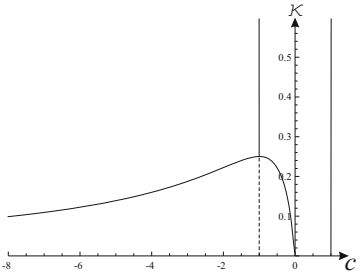

Fig. 7.8 Bifurcation of normal modes

A simple algebra reduces this to

$$(c-1)(c+1)[c+\kappa(c-1)^2]=0,$$

where $\kappa=\beta/\alpha$ is the coupling factor introduced previously. This algebraic equation has four roots

$$c=1,-1,1-\frac{1}{2\kappa}\pm\frac{1}{\kappa}\sqrt{1/4-\kappa}. \tag{7.10}$$

The last two roots are real only if $\kappa<1/4$. Thus, for $\kappa<1/4$ there are two additional normal modes bifurcated out of the antisymmetric mode $y=-x$ (vibrations in counterphases) at $\kappa=1/4$ as shown in Fig. 7.8, where the bold line denotes the stable modes and the dashed line the unstable one. This confirms also our observation with the Poincaré maps obtained previously by numerical integration.

Variational-Asymptotic Method. Since the normal symmetric and antisymmetric modes and the bifurcating modes found above are sensitive only to the coupling factor κ, we will consider the following variational problem: find the extremal of the functional

$$I[x(t),y(t)]=\frac{1}{2}\int_{t_0}^{t_1}[\dot{x}^2+\dot{y}^2-x^2-\frac{\varepsilon}{2}x^4-y^2-\frac{\varepsilon}{2}y^4-\frac{\varepsilon\kappa}{2}(y-x)^4]\,dt,$$

where ε is a small parameter and t_0 and t_1 are arbitrary time instants. We put for short $t_0=0$ and $t_1=T$. This action functional describes the coupled oscillators with two weakly nonlinear anchor springs and the weak coupling through the connecting nonlinear spring. It is convenient to change to the normal coordinates

$$u=\frac{1}{2}(x+y),\quad v=\frac{1}{2}(x-y).$$

Then the action functional becomes

$$I[u(t),v(t)]=\int_0^T[\dot{u}^2+\dot{v}^2-u^2-v^2-\frac{\varepsilon}{4}(u+v)^4-\frac{\varepsilon}{4}(u-v)^4-4\varepsilon\kappa v^4]\,dt. \quad (7.11)$$

To apply the variational-asymptotic method we put at the first step $\varepsilon=0$ to obtain

$$I_0[u(t),v(t)]=\int_0^T(\dot{u}^2+\dot{v}^2-u^2-v^2)\,dt.$$

This is the action functional describing vibrations of two uncoupled identical harmonic oscillators. The extremal is

$$u_0=A_1\cos t+B_1\sin t,\quad v_0=A_2\cos t+B_2\sin t, \quad (7.12)$$

for which the frequencies coincide so that the period T is 2π as expected.

As soon as $\varepsilon\neq 0$ the coefficients A_1, B_1, A_2, B_2 are becoming slightly dependent on time. Besides, taken for granted the bifurcation of modes for κ near $1/4$, we set $\kappa=1/4-\mu$ and look for the extremal at the second step in the two-timing fashion

$$u=A_1(\eta)\cos t+B_1(\eta)\sin t+u_1(t,\eta),$$
$$v=A_2(\eta)\cos t+B_2(\eta)\sin t+v_1(t,\eta),$$

where $\eta=\varepsilon t$ is the slow time. We assume that $u_1(t,\eta)$ and $v_1(t,\eta)$ are 2π-periodic functions with respect to the fast time t and are much smaller than u_0 and v_0 in the asymptotic sense. Note that the asymptotically principal terms of the time derivatives of u and v are

$$\dot{u}=u_{0,t}+\varepsilon u_{0,\eta}+u_{1,t},\quad \dot{v}=v_{0,t}+\varepsilon v_{0,\eta}+v_{1,t},$$

where the comma in indices denotes the partial derivatives. Substituting u, v and their derivatives into functional (7.11) and keeping the principal terms of u_1, v_1 and the principal cross terms between u_0, v_0 and u_1, v_1 we have

$$I_1[u_1(t),v_1(t)] = \int_0^{2\pi} [u_{1,t}^2 + v_{1,t}^2 + \underline{2u_{0,t}u_{1,t}} + \underline{2\varepsilon u_{0,\eta}u_{1,t}} + \underline{2v_{0,t}v_{1,t}} + \underline{2\varepsilon v_{0,\eta}v_{1,t}}$$
$$- (u_1^2 + v_1^2 + \underline{2u_0u_1} + \underline{2v_0v_1}) - \varepsilon(2u_0^3u_1 + 6u_0v_0^2u_1 + 6u_0^2v_0v_1$$
$$+ 2v_0^3v_1 + 16\kappa v_0^3v_1)]\,dt.$$

Integrating the third up to sixth terms by parts using the periodicity of u_1 and v_1 with respect to t, we see that the underlined terms gives $-4\varepsilon(u_{0,t\eta}u_1 + v_{0,t\eta}v_1)$. Then, substituting the expressions for u_0 and v_0 into the functional and reducing the products of sine and cosine to the sum of harmonic functions,[4] we get the resonant terms which should be removed in order to be consistent with the above asymptotic expansion. The equations obtained for A_1, B_1, A_2, B_2 read

$$\begin{aligned}
A_{1,\eta} &= \frac{3}{8}B_1(A_1^2+B_1^2) + \frac{3}{8}B_1(A_2^2+B_2^2) + \frac{3}{4}B_2(A_1A_2+B_1B_2),\\
B_{1,\eta} &= -\frac{3}{8}A_1(A_1^2+B_1^2) - \frac{3}{8}A_1(A_2^2+B_2^2) - \frac{3}{4}A_2(A_1A_2+B_1B_2),\\
A_{2,\eta} &= (\frac{3}{8}+3\kappa)B_2(A_2^2+B_2^2) + \frac{3}{8}B_2(A_1^2+B_1^2) + \frac{3}{4}B_1(A_1A_2+B_1B_2),\\
B_{2,\eta} &= -(\frac{3}{8}+3\kappa)A_2(A_2^2+B_2^2) - \frac{3}{8}A_2(A_1^2+B_1^2) - \frac{3}{4}A_1(A_1A_2+B_1B_2).
\end{aligned}$$

The above equations can still be simplified in terms of the variables a_1, a_2, and φ defined by

$$\begin{aligned}
A_1 &= a_1\cos\phi_1, \quad B_1 = a_1\sin\phi_1,\\
A_2 &= a_2\cos\phi_2, \quad B_2 = a_2\sin\phi_2,\\
\varphi &= \phi_2 - \phi_1.
\end{aligned} \tag{7.13}$$

According to these formulas a_1 and a_2 are the amplitudes of u and v, respectively, while φ is the phase difference modulo π. In terms of these new variables the equations of slow flow become (see exercise 7.7)

$$\begin{aligned}
a_{1,\eta} &= \frac{3}{8}a_1a_2^2\sin 2\varphi,\\
a_{2,\eta} &= -\frac{3}{8}a_1^2a_2\sin 2\varphi,\\
\varphi_{,\eta} &= -\frac{3}{8}(a_1^2+a_2^2) + 3\mu a_2^2 + \frac{3}{8}(a_2^2-a_1^2)\cos 2\varphi.
\end{aligned} \tag{7.14}$$

The Slow Flow. It follows from the first two equations of (7.14) that

$$\frac{da_1}{da_2} = -\frac{a_2}{a_1} \Rightarrow a_1^2 + a_2^2 = \rho^2,$$

[4] Again, this can be done with the TrigReduce command in *Mathematica*.

which means the conservation of the energy at this approximation, since terms of the order ε^2 and higher are neglected. This first integral enables one to reduce system (7.14) to two differential equations. Indeed, let us introduce a new variable ψ according to

$$a_1 = \rho\cos\psi, \quad a_2 = \rho\sin\psi, \tag{7.15}$$

with ρ being a constant in the above conservation law. Substituting these formulas into the first and the last equations of (7.14) we obtain

$$\begin{aligned} \psi_{,\eta} &= -\frac{3\rho^2}{16}\sin 2\varphi\sin 2\psi, \\ \varphi_{,\eta} &= -\frac{3\rho^2}{16}[8\mu(\cos 2\psi - 1) + 2 + 2\cos 2\psi\cos 2\varphi]. \end{aligned} \tag{7.16}$$

The obtained system of equations represents a slow flow on a two-dimensional torus, since the variables ψ and φ are modulo π.

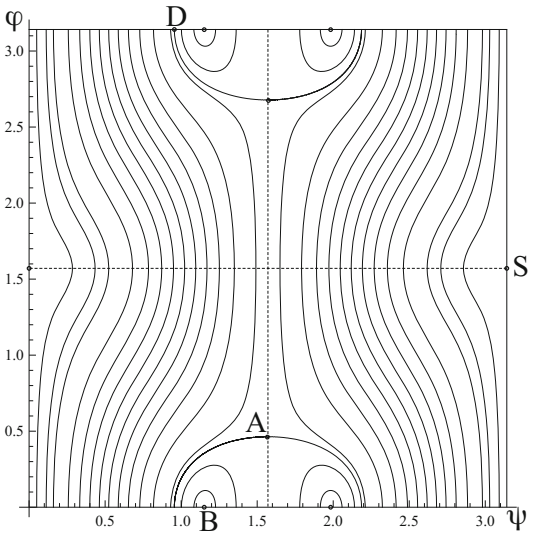

Fig. 7.9 Level curves of (7.17) for $\mu = 0.05$

In contrast to the original system (7.1), equations (7.16) can be integrated exactly. Indeed, by the straightforward differentiation we can easily verify that

$$-\frac{1}{2}\sin^2 2\psi\cos 2\varphi + (1-4\mu)\cos 2\psi + \mu\cos 4\psi = k \tag{7.17}$$

is the first integral of this slow flow, with k being a constant. The level curves of equation (7.17) are shown in Fig. 7.9 for $\mu = 0.05$. Each curve corresponds to a fixed value k of the first integral, but all are on the same energy level ρ^2. Due to the

periodicity in ψ points lying on the lines $\psi = 0$ and $\psi = \pi$ have to be identified. The same is true of φ. As a result, this figure represents the flow on the two-dimensional torus. Observe the symmetry with respect to the dashed lines $\varphi = \pi/2$ and $\psi = \pi/2$.

As we know, the nonlinear normal modes (7.10) found from the modal equation correspond to the fixed points of this flow. Let us first consider the symmetric normal mode for which $x = y$ and $v = 0$. In this case $A_2 = B_2 = 0$ and $a_2 = 0$, $a_1 = \rho$. Therefore $\psi = 0$ and the second equation of (7.16) implies that $\varphi = \pi/2$. Thus, this symmetric mode corresponds to the fixed point $(\psi, \varphi) = (0, \pi/2)$ (or $(\pi, \pi/2)$ denoted by S). We see that this mode is orbitally stable as the fixed point is a center surrounded by closed curves that result as intersections of invariant tori with the cut plane. For the antisymmetric normal mode we have $x = -y$ and $u = 0$. Therefore $a_1 = 0$ and consequently $\psi = \pi/2$. The second equation of (7.16) implies that $\varphi = \frac{1}{2}\arccos(1 - 8\mu)$. Thus, the antisymmetric normal mode is orbitally unstable as it is represented by the saddle points $(\psi, \varphi) = (\pi/2, \frac{1}{2}\arccos(1 - 8\mu))$ (point A) and $(\psi, \varphi) = (\pi/2, \pi - \frac{1}{2}\arccos(1 - 8\mu))$. The homoclinic orbits are the closed curves starting and ending at these saddle points.[5] The bifurcating modes satisfy the relations $u = \frac{1}{2}(1 + c)x$ and $v = \frac{1}{2}(1 - c)x$, so u and v are proportional and the phase difference φ must be zero. It follows from the second equation of (7.16) that $\psi = \frac{1}{2}\arccos\frac{4\mu-1}{4\mu+1}$ or $\psi = \pi - \frac{1}{2}\arccos\frac{4\mu-1}{4\mu+1}$. We see that these bifurcating modes are orbitally stable (since they appear as centers) and correspond to the fixed points $(\psi, \varphi) = (\frac{1}{2}\arccos\frac{4\mu-1}{4\mu+1}, 0)$ (point B) and $(\psi, \varphi) = (\pi - \frac{1}{2}\arccos\frac{4\mu-1}{4\mu+1}, 0)$, respectively.

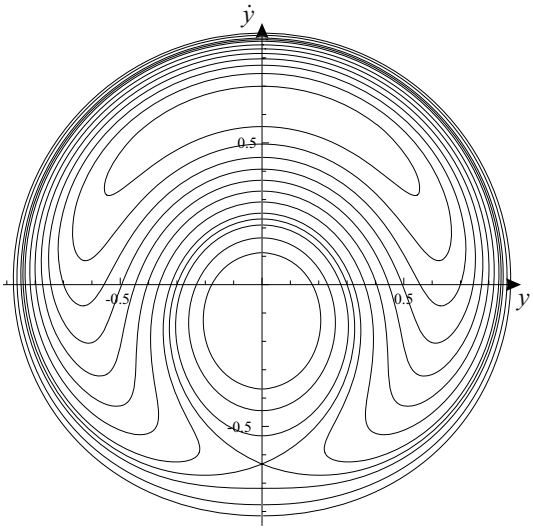

Fig. 7.10 Poincaré map according to approximate theory for $E_0 = 0.4$ and $\mu = 0.15$

[5] See the detailed analysis of the homoclinic motion in [49].

Comparison with Numerical Simulations. The comparison with the Poincaré map constructed numerically in the previous Section is possible if we express the results obtained for u and v in terms of the "old" coordinates x and y

$$x = u + v, \quad y = u - v.$$

To compute the approximate Poincaré map we must set $x = 0$

$$x = u_0 + v_0 + O(\varepsilon) = 0,$$

so, taking into account (7.12) we have

$$\tan t = -\frac{A_2(\eta) + A_1(\eta)}{B_2(\eta) + B_1(\eta)}.$$

Finding from here $\sin t$ and $\cos t$ and substituting into $y = u_0 - v_0$ we obtain

$$y = \frac{2(B_1A_2 - A_1B_2)}{(B_2^2 + 2B_1B_2 + A_2^2 + 2A_1A_2 + B_1^2 + A_1^2)^{1/2}},$$

where the argument η from A_1, B_1, A_2, B_2 is omitted. The velocity $\dot{y}$, to the lowest order of approximation in ε, is

$$\dot{y} = y_{,t} = \frac{B_2^2 + A_2^2 - B_1^2 - A_1^2}{(B_2^2 + 2B_1B_2 + A_2^2 + 2A_1A_2 + B_1^2 + A_1^2)^{1/2}}.$$

In terms of the angles φ and ψ introduced in (7.13) and (7.15) the formulas for y and $\dot{y}$ read

$$y = \frac{\rho \sin\varphi \sin 2\psi}{\sqrt{1 + \cos\varphi \sin 2\psi}}, \quad \dot{y} = \frac{\rho \cos 2\psi}{\sqrt{1 + \cos\varphi \sin 2\psi}}.$$

To construct the approximate Poincaré map we must use the first integral (7.17) to find $\cos 2\varphi$ for the given values of μ, k, ρ, and ψ. Then plugging the obtained values of φ into the above formulas to evaluate y and $\dot{y}$ and to plot the curve in the cut plane. The total energy E_0 of the system is related to ρ by the expression $E_0 = \rho^2$. The approximate Poincaré map corresponding to the energy level $E_0 = 0.4$ and to the coupling factor $\kappa = 0.1$ ($\mu = 0.15$) is shown in Fig. 7.10. It is seen that both maps in Fig. 7.7 (left) and Fig. 7.10 coincide qualitatively.

To show the quantitative agreement let us compute the Poincaré map for $E_0 = 0.4$, $\varepsilon = 0.1$, and $\mu = 0.15$, and for a solution satisfying the following initial conditions

$$x(0) = 0, \quad y(0) = 0, \quad \dot{y}(0) = -0.65.$$

Then it is easy to find that $k = -0.2519$. The comparison of Poincaré maps obtained by the numerical integration (points) and by the approximate theory (bold line) is shown in Fig. 7.11 (see exercise 7.8). The agreement is really palpable, although $\varepsilon = 0.1$ is not quite small.

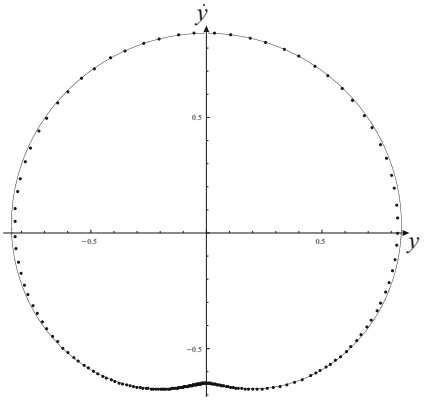

Fig. 7.11 Comparison of Poincaré maps for $E_0 = 0.4$, $\varepsilon = 0.1$, and $\kappa = 0.1$

7.3 KAM Theory

The perturbation theory of quasiperiodic motions of conservative mechanical systems [5, 25] proposed by Kolmogorov, Arnold, and Moser, called for short KAM theory, is perhaps one of the greatest achievements in mathematics and mechanics of the 20th century. It has a lot of consequences and applications in dynamics and also in statistical mechanics. Although the ideas upon which the theory is based seem quite simple, the detailed proofs presented in the mathematical literature have been for long time serious barriers for people with the engineering background. This Section aims at explaining KAM theory with the variational-asymptotic method.

Variational Problem. Our starting point is Hamilton's variational principle, according to which motions of any conservative mechanical system correspond to extremals of the action functional

$$I[q(t)] = \int_{t_0}^{t_1} L(q,\dot{q})\,dt, \tag{7.18}$$

where $q(t) = (q_1(t),\dots,q_n(t))$. As we know, this implies Lagrange's equations

$$\frac{d}{dt}\frac{\partial L}{\partial \dot{q}_j} - \frac{\partial L}{\partial q_j} = 0, \quad j = 1,\dots,n.$$

Suppose that the Lagrange function has the form

$$L(q,\dot{q}) = L_0(q,\dot{q}) + \varepsilon L_1(q,\dot{q}),$$

where ε is a small parameter. Besides, we assume for simplicity that $L(q,\dot{q})$ is an analytic function and that the determinant $\det L_{,\dot{q}\dot{q}}$ is positive everywhere. The problem is to study the asymptotic behavior of the extremals depending on this small

parameter ε. Note that the number n of degrees of freedom must be at least 2 since systems with one degree of freedom are always integrable leading to the periodic extremals for small energies.

First Step. Since the action functional (7.18) contains a small parameter, it is natural to use the variational-asymptotic method to analyze it. At the first step of the variational-asymptotic method we neglect the small term $\varepsilon L_1(q,\dot{q})$ and consider instead the variational problem: find the extremal of the functional

$$I_0[q(t)] = \int_{t_0}^{t_1} L_0(q,\dot{q})\,dt.$$

This leads to Lagrange's equations

$$\frac{d}{dt}\frac{\partial L_0}{\partial \dot{q}_j} - \frac{\partial L_0}{\partial q_j} = 0. \tag{7.19}$$

We assume that Lagrange's equations (7.19) are integrable so that their solutions can be found at this step. Such situation is met by the nonlinear coupled mass-spring oscillators considered in example 7.1 if the coupling parameter β is set to be zero. In this case the system reduces to two uncoupled nonlinear oscillators, each of which has only one degree of freedom.

As equations (7.19) are integrable, there exist angle-action variables (φ, I) in terms of which the unperturbed Hamilton function becomes independent of φ: $H_0 = H_0(I)$ (see Section 7.1 and [5]). The solution of Hamilton's equations

$$\dot{\varphi}_j = \frac{\partial H_0}{\partial I_j} = \omega_j(I_j), \quad \dot{I}_j = -\frac{\partial H_0}{\partial \varphi_j} = 0,$$

which are equivalent to (7.19), is quite simple in these variables: $\varphi_j = \varphi_{j0} + \omega_j t$ and $I_j = \text{const}$. Coming back to $q(t)$, the solution of (7.19) can be presented in the form

$$q(t) = q_0(t) = u_0(\varphi_0 + \omega t),$$

where $u_0(\varphi)$ is the vector-valued function of $\varphi = (\varphi_1, \ldots, \varphi_n)$ which is periodic in each variable φ_j with the period 2π, and $\omega = (\omega_1, \ldots, \omega_n)$ are the constant frequencies. Thus, every solution is now quasi-periodic in t: its frequency spectrum in general does not consist of integer multiples of a single frequency as in the case with periodic solutions, but rather of integer combinations of a finite number of different frequencies.[6] For fixed φ_0 function $u_0(\varphi_0 + \omega t)$ describes a curve winding around some invariant n-dimensional torus T^n with winding numbers, $\omega = (\omega_1, \ldots, \omega_n)$. Mention that $u_0(\varphi)$ is a differentiable one-to-one map which maps the invariant torus onto itself. We shall use angle variables $\varphi = (\varphi_1, \ldots, \varphi_n)$, each is modulo 2π,

[6] In this sense, the asymptotic analysis provided here is multi-frequency analysis, which is much more difficult than all previous asymptotic analyses due to the problem of small divisors.

as coordinates on the torus. All solutions with fixed I_j belong to one torus, so that the whole phase space is foliated into an n-parameter family of invariant tori.

The flow on each torus depends on the arithmetical properties of its frequencies ω_j. There are essentially two cases.

i) The frequencies ω_j are non-resonant, i.e., $k \cdot \omega \neq 0$ for all non-zero $k = (k_1, \ldots, k_n)$, with k_j being integers (we write $k \in \mathbb{Z}^n$). Then each orbit is dense on this torus.

ii) The frequencies ω_j are resonant, that is, there exist integer relations $k \cdot \omega = 0$ for some non-zero $k \in \mathbb{Z}^n$. In this case each orbit is dense on some lower dimensional torus, but not in T^n.

We assume that the unperturbed system is non-degenerate in the sense that

$$\det \left| \frac{\partial^2 H_0}{\partial I_i \partial I_j} \right| \neq 0.$$

In this case the frequencies ω_j depend on the amplitudes, so they vary with the torus. This nonlinear frequency-amplitude relation is essential for the stability results of the KAM theory. It follows that the subset of non-resonant tori as well as that of resonant tori form dense subsets in phase space. Similar to the set of real numbers, the resonant tori sit among the non-resonant ones like the rational numbers among the irrational numbers.

Small Perturbations and KAM Theorem. Let us include now the small term $\varepsilon L_1(q, \dot{q})$ into the action functional and consider the perturbed variational problem. The first result, obtained already by Poincaré, showed that the resonant tori are in general destroyed by an arbitrarily small perturbation. In particular, out of a torus with an $n-1$-parameter family of periodic orbits, usually only finitely many periodic orbits survive a small perturbation, while the others disintegrate and give way to chaotic behavior. Since a set of resonant tori being destroyed by a small perturbation is dense among all invariant tori, there seems to be no hope for other tori to survive. In fact, until the middle of the 20th century it was a common belief that arbitrarily small perturbations can turn an integrable system into an ergodic one on each energy surface. By the way, it would not help if the non-degeneracy assumption is dropped. There exists a counter-example showing that if H_0 is too degenerate, the motion may even become ergodic on each energy surface, thus destroying all tori.

Kolmogorov [25] was the first to observe that, for the non-degenerate case, the converse is true: the majority of tori survives small perturbations. He gave the sketch of the proof about the persistence of those tori, whose frequencies ω_j are not only non-resonant, but are strongly non-resonant in the sense that there exist constants $\alpha > 0$ and $\nu > 0$ such that

$$|k \cdot \omega| \geq \frac{\alpha}{|k|^\nu} \tag{7.20}$$

for all non-zero $k \in \mathbb{Z}^n$, where $|k| = |k_1| + \ldots + |k_n|$. Condition (7.20) is called a diophantine or small divisor condition. It turns out that the set of strongly non-resonant frequencies for any fixed $\nu > n-1$ has the full measure, in contrast to the set of remaining frequencies having zero measure. But although almost all frequencies are

strongly non-resonant, it is not true that almost all tori survive a given perturbation εL_1, no matter how small ε is. In its precise formulation, KAM theorem states that there exists a constant $\delta > 0$ such that for the perturbations of size $|\varepsilon| < \delta\alpha^2$ the strongly non-resonant tori of the unperturbed system persist, being only slightly deformed. Moreover, they depend continuously on ω and fill the phase space up to a set of measure $O(\alpha)$. An immediate consequence of the KAM theorem, important for the statistical mechanics, is that small perturbations of integrable systems do not necessarily imply ergodicity, as the invariant tori form a set, which is neither of full nor of zero measure. It has to be emphasized, however, that this invariant set, although of large measure, is a Cantor set and thus has no interior points. It is therefore impossible to tell with finite precision whether a given initial condition falls onto an invariant torus or into a gap between such tori. From a physical point of view the KAM theorem rather makes a probabilistic statement: with overwhelming probability of order $1 - O(\alpha)$ a randomly chosen orbit lies on an invariant torus and thus stays there forever.

Variational Problem for Invariant Tori. Since for an invariant torus with fixed frequencies ω the solution of Lagrange's equations has the form $q(t) = u(\varphi_0 + \omega t)$, the generalized velocities may be written as

$$\dot{q} = \sum_{j=1}^{n} \omega_j \frac{\partial}{\partial \varphi_j} u = \nabla u,$$

where ∇ denotes the linear first order partial differential operator with constant coefficients

$$\nabla = \sum_{j=1}^{n} \omega_j \frac{\partial}{\partial \varphi_j}.$$

Therefore it is convenient to consider the following variational problem for an invariant torus, first mentioned in [39]: find extremals of the functional

$$I[u(\varphi)] = \int_0^{2\pi} \dots \int_0^{2\pi} L(u, \nabla u)\, d\varphi_1 \dots d\varphi_n = \int_{T^n} L(u, \nabla u)\, d\varphi \tag{7.21}$$

among vector-valued functions $u(\varphi) = (u_1(\varphi), \dots, u_n(\varphi))$ which are 2π-periodic in each variable φ_j. Euler-Lagrange's equations of this variational problem read

$$\nabla L_{,\dot{q}}(u, \nabla u) - L_{,q}(u, \nabla u) = 0. \tag{7.22}$$

Thus, instead of solving the ordinary differential equations, we have to deal now with the nonlinear partial differential equations (7.22). Conversely, every solution $u(\varphi)$ of (7.22), 2π-periodic in each variable φ_j, determines the flow on some invariant torus which satisfies original Lagrange's equations. We shall therefore apply the variational-asymptotic method to the variational problem (7.21). Then it is easy to see that the first step of the variational-asymptotic procedure leads to the unperturbed problem

$$\nabla L_{0,\dot{q}}(u,\nabla u) - L_{0,q}(u,\nabla u) = 0,$$

and, consequently, to the flow on the unperturbed invariant torus induced by the solution $u_0(\varphi)$ of this equation.

Second Step and Sketch of the Proof. In order to justify KAM theorem[7] let us proceed to the second step of the variational-asymptotic method. We fix the solution of the unperturbed problem on some torus, $u_0(\varphi)$, and look for the extremal of (7.21) in the form

$$u(\varphi) = u_0(\varphi) + u_1(\varphi),$$

where $u_1(\varphi)$ is smaller than $u_0(\varphi)$ in the asymptotic sense. Substituting this into the action functional (7.21), expanding the Lagrangian in the Taylor series, and keeping the asymptotically principal terms containing u_1, we obtain

$$I_1[u_1(\varphi)] = \int_{T^n} [L_{,q}|_0 \cdot u_1 + L_{,\dot{q}}|_0 \cdot \nabla u_1 + \frac{1}{2}(u_1 \cdot L_{,qq}|_0 u_1 + u_1 \cdot L_{,\dot{q}q}|_0 \nabla u_1 + \nabla u_1 \cdot L_{,q\dot{q}}|_0 u_1 + \nabla u_1 \cdot L_{,\dot{q}\dot{q}}|_0 \nabla u_1)]\, d\varphi.$$

The vertical bar followed by index 0 means that the derivatives in front of it have to be evaluated at $(u_0(\varphi), \nabla u_0(\varphi))$. Thus, these first and second derivatives become functions of φ which are the coordinates on the torus. The obtained functional turns out to be quadratic with respect to u_1. Its Euler-Lagrange's equation is linear and can be presented in the form

$$E(u_0) + dE(u_0)u_1 = 0, \tag{7.23}$$

where

$$E(u) = \nabla L_{,\dot{q}}(u,\nabla u) - L_{,q}(u,\nabla u), \tag{7.24}$$

and

$$dE(u_0)u_1 = \nabla(L_{,\dot{q}\dot{q}}|_0 \nabla u_1) + (L_{,\dot{q}q}|_0 - L_{,q\dot{q}}|_0)\nabla u_1 + (\nabla L_{,\dot{q}q}|_0 - L_{,qq}|_0)u_1. \tag{7.25}$$

It is interesting to mention that

$$dE(u)v = \frac{d}{d\lambda} E(u + \lambda v)|_{\lambda=0},$$

so equation (7.23) resembles Newton's iteration method of finding the root of a transcendental equation or the minimum of a function [41]. According to the variational-asymptotic method we can also replace L in (7.25) by L_0 which makes the error in determining u_1 of the order ε compared with 1. Since our aim is not computing u_1, but just proving the existence of the solution, we keep (7.25) to be exactly as in Newton's iteration procedure.

[7] See the rigorous and detailed proof in [46].

One of the difficulties in solving equation (7.23) comes from the linear operator ∇ in (7.25). Due to the small divisors, entering the representation of this operator with respect to the Fourier expansion of functions on the torus, its inverse is unbounded. Indeed, let us consider an equation $\nabla u = g$, where functions u and g are 2π periodic in each variable φ_j and can therefore be presented in terms of the Fourier series

$$u(\varphi) = \sum_{k\in\mathbb{Z}^n} u_k e^{ik\cdot\varphi}, \quad g(\varphi) = \sum_{k\in\mathbb{Z}^n} g_k e^{ik\cdot\varphi}.$$

Applying the operator ∇ to u, we get

$$\nabla u = \sum_{j=1}^{n} \omega_j \frac{\partial}{\partial\varphi_j} u = \sum_{k\in\mathbb{Z}^n} i(k\cdot\omega) u_k e^{ik\cdot\varphi},$$

so that the equation $\nabla u = g$ becomes

$$\sum_{k\in\mathbb{Z}^n} i(k\cdot\omega) u_k e^{ik\cdot\varphi} = \sum_{k\in\mathbb{Z}^n} g_k e^{ik\cdot\varphi}.$$

Even for non-resonant frequencies the combinations $k\cdot\omega$ may become arbitrarily small leading to the unbounded coefficients u_k of the series. The diophantine condition (7.20) has been introduced to remove infinitely small divisors. Now it is straightforward to show that for ω satisfying condition (7.20) and for every regular function $g(\varphi)$ with zero mean value, the equation $\nabla u = g$ has a unique solution with zero mean value. Indeed, since the Fourier series for $g(\varphi)$ converges, the coefficients g_k satisfy the following conditions

$$|g_k| \le a\rho^{|k|}$$

with some positive a and $\rho < 1$. Besides, $g_0 = 0$ as $\mathbf{g}(\varphi)$ has the zero mean value. Then $u_0 = 0$, $u_k = g_k/(ik\cdot\omega)$ and the Fourier series

$$u(\varphi) = \sum_{k\neq 0} \frac{g_k}{i(k\cdot\omega)} e^{ik\cdot\varphi}$$

clearly converges on account of the diophantine condition (7.20). The norm of $u(\varphi)$ can be precisely estimated.

But there are still two more obstacles to solving equation (7.23). First, the terms containing u_1 and ∇u_1 in equation (7.25) have to be eliminated. Then, the remaining second order partial differential equation requires a compatibility condition, namely that the inhomogeneous term $E(u_0)$ be of zero mean value. Note that these obstacles disappear in the special case when the identity map $u_0 = \varphi$ is an approximate solution of $E(u_0) = 0$. In this case it is easy to check that the coefficient matrices of u_1 and ∇u_1 in (7.25) are small and can be neglected. Indeed, the coefficient matrix of u_1 is the Jacobian matrix of $E(\varphi)$. For the estimation of the coefficient matrix of ∇u_1 we refer to the subsequent formula $(7.29)_1$. Therefore equation (7.23) can be replaced by

$$\nabla(L_{,\dot{q}\dot{q}}|_0 \nabla u_1) = -E(\varphi)$$

and, by the above arguments, it can be solved since the right-hand side must always be of zero mean value. We conclude that, if the identity map $u_0 = \varphi$ is an approximate solution of $E(u_0) = 0$, then (7.23) admits an approximate solution u_1 so that the first step of the Newton iteration can be performed in this case.

Now the following idea allows us to reduce the general case to the one where u_0 is the identity map on the torus: let us try to *change* the Lagrangian so that the changed Euler-Lagrange's equation admits the identity map as solution. Consider the group of one-to-one maps $u(\varphi)$ of the torus which acts on the space of Lagrangians L according to the rule

$$u^*L(\varphi, v) = L(u(\varphi), Uv),$$

where $U(\varphi) = \partial u/\partial\varphi$ denotes the Jacobian matrix of u and is therefore 2π-periodic in each variable φ_j. Here u^*L is regarded as a function of the formal arguments φ and v, with v playing the role of the velocity. One verifies easily that

$$(u \circ v)^*L = u^*(v^*L), \quad id^*L = L,$$

where $(u \circ v)(\varphi) = u(v(\varphi))$ corresponds to the composition of two maps and id is the identity map $id = \varphi$. Functional (7.21) is compatible with this group action in the sense that

$$I_L[u \circ v(\varphi)] = I_{u^*L}[v(\varphi)],$$

and, moreover, it is invariant under the subgroup of translations. Since the Lagrangian may change, we attach it as the index to the functional. Taking the variation of the functionals standing on both sides, we find that

$$(U(v))^T E(L, u \circ v) = E(u^*L, v),$$

with $E(L,u)$ being the expression (7.24) where the Lagrangian is indicated precisely. Differentiating this equation with respect to v in the direction of a tangent vector w to the group of maps at $v = id$, we obtain

$$U^T dE(L,u)Uw = dE(u^*L, id)w - (dU \cdot w)^T E(L,u) \tag{7.26}$$

The previous equation with $v = id$ reduces to

$$U^T E(L,u) = E(u^*L, id). \tag{7.27}$$

It now follows from (7.27) that whenever u is an approximate solution of $E(L,u) = 0$ then also $E(u^*L, id)$ is small and hence the above considerations about the case $u = id$ show that there exists an approximate solution w of the equation $dE(u^*L, id)w = -E(u^*L, id)$. Combining this observation with the identities (7.26) and (7.27), we conclude that equation (7.23) indeed has an approximate solution $u_1 = U_0 w$ in the sense that errors of quadratic order are ignored.

The precise estimation for the approximate solution of the linearized equation (7.23) are based on several formulas which are summarized below. First,

$$U^T dE(L,u)Uw = \nabla(A\nabla w) + B\nabla w + Cw, \tag{7.28}$$

where A, B, and C are the $n \times n$ matrix-valued functions on T^n defined by

$$A = U^T L_{,vv} U, \quad B = U^T L_{,v\varphi} - L^T_{,v\varphi} U, \quad C = U^T E_{,\varphi},$$

and the following abbreviations are used

$$L_{,v\varphi} = \frac{\partial}{\partial \varphi} L_{,v}(u(\varphi), \nabla u(\varphi)), \quad E_{,\varphi} = \frac{\partial}{\partial \varphi} E(L,u), \quad U = \frac{\partial u}{\partial \varphi}.$$

Formula (7.28) follows from equation (7.26) by inserting the expression (7.25) with L and u_1 replaced by u^*L and w, respectively. Then we have

$$\begin{aligned} \nabla B &= C - C^T, \\ \int_{T^n} B\, d\varphi &= 0, \\ \int_{T^n} U^T E(L,u)\, d\varphi &= 0. \end{aligned} \tag{7.29}$$

Formula $(7.29)_1$ expresses the fact, well known in variational calculus, that the operator

$$Mw = \nabla(A\nabla w) + B\nabla w + Cw,$$

which represents the Hessian of the functional (7.21), is self-adjoint. Indeed, since $A^T = A$ and $B^T = -B$, the adjoint operator of M is given by

$$M^* w = \nabla(A^T \nabla w) - \nabla(B^T w) + C^T w = \nabla(A\nabla w) + B\nabla w + (C^T + \nabla B)w$$

so that $M^* = M$ if and only if $C^T + \nabla B = C$.

The last two formulas reflect the fact that the functional $I[u(\varphi)]$ defined by (7.21) is invariant under the subgroup of translations of the torus T^n (see exercise 7.9).

It follows from these formulas that if u is a solution of $E(L,u) = 0$ and the frequency vector ω is rationally independent then $C = 0$ and $B = 0$. Indeed, since $\nabla B = 0$ the function $B(\varphi)$ is constant along the dense line $\varphi = \omega t$. Hence it is constant on T^n and it follows from $(7.29)_2$ that $B = 0$. As a consequence the linearized operator is given by

$$U^T dE(L,u)Uw = \nabla(A\nabla w)$$

which is invertible.

Provided u_1 can be found and the error we make can be estimated, we now replace u_0 by $u_0 + u_1$ and *repeat* the second step of the variational-asymptotic procedure to find the next correction. This is the crucial idea of Newton's iteration leading to the fast convergence. It can simply be shown in the case of finding roots of transcendental equations that if the initial error is ε, then the error after n iteration would be of the order ε^{2^n}. Such fast convergence, valid also for (7.23) as shown in [46], may remove the errors induced by the small divisors at each iteration and guarantees the convergence to the solution of variational problem (7.21).

7.4 Coupled Self-excited Oscillators

As we know, a self-excited oscillator, such as van der Pol's oscillator, may generate a limit cycle periodic vibration with a fixed frequency. What happens if two slightly different self-excited oscillators are coupled? One may imagine for instance two violins playing near each other and interacting through the sound wave, or two Froude's pendulums connected by a weak spring. Another example is two pendulum clocks which move into the same swinging rhythm when they are hung near each other on the wall. Although uncoupled oscillators have in general different frequencies, the effect of the coupling may lead to a vibration which is phase and frequency locked, or in another word, to synchronization.[8]

Two Weakly Coupled van der Pol's Oscillators. We will study the synchronization of two weakly coupled van der Pol's oscillators, whose Lagrange function is given by

$$L(x,y,\dot{x},\dot{y}) = \frac{1}{2}(\dot{x}^2+\dot{y}^2) - \frac{1}{2}[x^2+(1+\varepsilon\alpha)y^2+\varepsilon\kappa(x-y)^2],$$

where ε is a small parameter, parameter α characterizes the difference in uncoupled frequencies, while κ is a coupling factor. Since we are interested in the primary resonance, we order the amplitude of the coupling to be the same as the damping and non-linear term [10]. Thus, the dissipation function assumes the form

$$D(x,y,\dot{x},\dot{y}) = \frac{1}{2}\varepsilon[(x^2-1)\dot{x}^2+(y^2-1)\dot{y}^2].$$

Then $x(t)$ and $y(t)$ satisfy the variational equation

$$\delta\int_{t_0}^{t_1} L(x,y,\dot{x},\dot{y})\,dt - \int_{t_0}^{t_1}(\frac{\partial D}{\partial\dot{x}}\delta x+\frac{\partial D}{\partial\dot{y}}\delta y)\,dt = 0.$$

Generalized Lagrange's equations read [10]

$$\begin{aligned} \ddot{x}+x+\varepsilon\kappa(x-y)-\varepsilon(1-x^2)\dot{x} &= 0,\\ \ddot{y}+(1+\varepsilon\alpha)y-\varepsilon\kappa(x-y)-\varepsilon(1-y^2)\dot{y} &= 0. \end{aligned} \tag{7.30}$$

We need to find the asymptotic behavior of solution in the limit $\varepsilon\to 0$.

When $\kappa = 0$ the system (7.30) is uncoupled and the two equations exhibit unsynchronized limit cycle vibrations for $x(t)$ and $y(t)$ with different frequencies 1 and $\sqrt{1+\varepsilon\alpha}$. When κ is small, then we may expect by the continuity reasoning that the vibrations are still unsynchronized. For finite κ we may have three states of a coupled self-organized oscillator: strongly locked, weakly locked, and unlocked. The vibration is said to be strongly locked (or strongly synchronized) if it is both frequency and phase locked. If the vibration is frequency locked but the relative phase

[8] The earliest known observation of synchronization was made by Huygens. He reported that "two clocks, hanging side by side and separated by one or two feet, keep between them a consonance so exact that the two pendula always strike together, never varying".

changes slowly with time, it is called weakly locked (or weakly synchronized). If the frequencies of vibration are different, the system is said to be unlocked or drifting.

Numerical Solutions. The system of equations (7.30) does not admit exact analytical solutions. So, in order to observe the behavior of solutions and to illustrate the difference between synchronized and unsynchronized vibrations let us first do some numerical simulations.

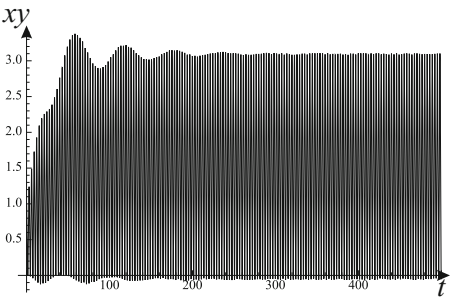

Fig. 7.12 Graph $x(t)y(t)$ of coupled van der Pol's oscillators for $\varepsilon = 0.1$, $\alpha = 1$, and $\kappa = 1.2$

We take for example $\varepsilon = 0.1$, $\alpha = 1$, and $\kappa = 1.2$ and find the solution to (7.30) satisfying the initial conditions $x(0) = 1$, $\dot{x}(0) = 0$ and $y(0) = 1$, $\dot{y}(0) = 0$ by the numerical integration with *Mathematica*. The plot of the product $x(t)y(t)$ shown in Fig. 7.12 exhibits obviously synchronization in this case. Indeed, since $x(t)$ and $y(t)$ approach periodic (for small ε harmonic) functions with the same frequency and constant phase difference, their product must have a steady-state character after a short transient period.

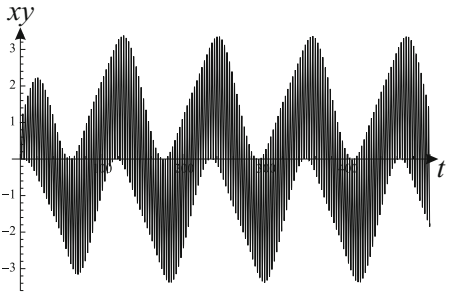

Fig. 7.13 Graph $x(t)y(t)$ of coupled van der Pol's oscillators for $\varepsilon = 0.1$, $\alpha = 1$, and $\kappa = 0.5$

If we decrease the coupling factor while keeping all other parameters and initial data, the response may change drastically. For example, the plot of the product $x(t)y(t)$ for $\kappa = 0.5$ shown in Fig. 7.13 does not indicate vibrations of $x(t)$ and $y(t)$

with equal frequency and constant phase difference. Thus, in this case synchronization does not occur, and the system is unlocked.

In the next paragraph we will use the variational-asymptotic method to establish the law of slow change of amplitudes and phases as function of the frequency difference and the coupling parameter and to predict the synchronization.

Variational-Asymptotic Method. Let us introduce the frequency ω of vibration precisely into the variational equation by multiplying it with ω and rewriting in terms of the stretched angular time $\tau = \omega t$ for one fix period 2π

$$\begin{aligned}\delta \int_{\tau_0}^{\tau_0+2\pi} \{\frac{1}{2}\omega^2(x'^2+y'^2) - \frac{1}{2}[x^2+(1+\varepsilon\alpha)y^2+\varepsilon\kappa(x-y)^2]\}\,d\tau \\ + \int_{\tau_0}^{\tau_0+2\pi} \varepsilon\omega[(1-x^2)x'\delta x + (1-y^2)y'\delta y]\,d\tau = 0,\end{aligned} \tag{7.31}$$

where prime denotes the derivative with respect to τ and τ_0 is an arbitrary time instant. We write for short $\tau_0 = 0$.

We put at the first step $\varepsilon = 0$ to obtain

$$\delta \int_0^{2\pi} [\frac{1}{2}\omega^2(x'^2+y'^2) - \frac{1}{2}(x^2+y^2)]\,d\tau = 0.$$

The 2π-periodic extremal is

$$x_0 = A_1\cos\tau + B_1\sin\tau, \quad y_0 = A_2\cos\tau + B_2\sin\tau, \tag{7.32}$$

for which the frequency ω is equal to 1 as expected.

As soon as $\varepsilon \neq 0$ the coefficients A_1, B_1, A_2, B_2 are becoming slightly dependent on time and ω deviates from 1. Therefore we look for the extremal and for the frequency at the second step in the form

$$\begin{aligned}x &= A_1(\eta)\cos\tau + B_1(\eta)\sin\tau + x_1(\tau,\eta),\\ y &= A_2(\eta)\cos\tau + B_2(\eta)\sin\tau + y_1(\tau,\eta), \quad \omega = 1+\omega_1,\end{aligned}$$

where $\eta = \varepsilon\tau$ is the slow time. We assume that $x_1(\tau,\eta)$ and $y_1(\tau,\eta)$ are 2π-periodic functions with respect to the fast time τ and are much smaller than x_0 and y_0 in the asymptotic sense, and ω_1 is much smaller than 1. Note that the asymptotically principal terms of the derivatives of x and y are

$$x' = x_{0,\tau} + \varepsilon x_{0,\eta} + x_{1,\tau}, \quad y' = y_{0,\tau} + \varepsilon y_{0,\eta} + y_{1,\tau},$$

where the comma in indices denotes the partial derivatives. Substituting x, y together with their derivatives into functional (7.31) and keeping the principal terms of x_1, y_1 and the principal cross terms between x_0, y_0 and x_1, y_1 we have

$$\delta\int_0^{2\pi}\{\frac{1}{2}x_{1,\tau}^2+\frac{1}{2}y_{1,\tau}^2+\underline{x_{0,\tau}x_{1,\tau}}+\underline{\varepsilon x_{0,\eta}x_{1,\tau}}+\underline{2\omega_1 x_{0,\tau}x_{1,\tau}}+\underline{y_{0,\tau}y_{1,\tau}}+\underline{\varepsilon y_{0,\eta}y_{1,\tau}}$$
$$+\underline{2\omega_1 y_{0,\tau}y_{1,\tau}}-(\frac{1}{2}x_1^2+\frac{1}{2}y_1^2+\underline{x_0x_1}+\underline{y_0y_1})-\varepsilon[\alpha y_0y_1+\kappa(x_0-y_0)(x_1-y_1)$$
$$-(1-x_0^2)x_{0,\tau}x_1-(1-y_0^2)y_{0,\tau}y_1]\}\,d\tau=0.$$

Integrating the third up to eighth terms by parts using the periodicity of x_1 and y_1 with respect to τ, we see that the underlined terms gives $-2\varepsilon(x_{0,\tau\eta}x_1+y_{0,\tau\eta}y_1)+2\omega_1(x_0x_1+y_0y_1)$. Then, substituting the expressions for x_0 and y_0 into the functional and reducing the products of sine and cosine to the sum of harmonic functions, we get the resonant terms which should be removed in order to be consistent with the above asymptotic expansion. This implies that ω_1 must be of the order ε; let us denote it by $\omega_1=\varepsilon k_1$. The equations obtained for A_1, B_1, A_2, B_2 read[9]

$$2A_{1,\eta}=-2k_1B_1+A_1-\frac{A_1}{4}(A_1^2+B_1^2)+\kappa(B_1-B_2),$$
$$2B_{1,\eta}=2k_1A_1+B_1-\frac{B_1}{4}(A_1^2+B_1^2)+\kappa(A_2-A_1),$$
$$2A_{2,\eta}=-2k_1B_2+\alpha B_2+A_2-\frac{A_2}{4}(A_2^2+B_2^2)+\kappa(B_2-B_1),$$
$$2B_{2,\eta}=2k_1A_2-\alpha A_2+B_2-\frac{B_2}{4}(A_2^2+B_2^2)+\kappa(A_1-A_2).$$

This system of equations can still be simplified if we introduce the amplitudes and phases of vibrations in accordance with

$$A_1=a_1\cos\phi_1,\quad B_1=a_1\sin\phi_1,$$
$$A_2=a_2\cos\phi_2,\quad B_2=a_2\sin\phi_2.$$

Thus, a_1 and a_2 characterize the amplitudes of x_0 and y_0, respectively, while ϕ_1 and ϕ_2 are the corresponding phases.

In terms of the new variables the equations that result from the elimination of the resonant terms can be written as

$$2a_{1,\eta}=a_1(1-\frac{a_1^2}{4})+\kappa a_2\sin(\phi_1-\phi_2),$$
$$2a_{2,\eta}=a_2(1-\frac{a_2^2}{4})-\kappa a_1\sin(\phi_1-\phi_2),$$
$$2\phi_{1,\eta}=2k_1-\kappa+\frac{\kappa a_2\cos(\phi_1-\phi_2)}{a_1},$$
$$2\phi_{2,\eta}=2k_1-\alpha-\kappa+\frac{\kappa a_1\cos(\phi_1-\phi_2)}{a_2}.$$

[9] One may check this with the TrigReduce command in *Mathematica*.

Introducing the phase difference $\varphi = \phi_1 - \phi_2$, we reduce this system further to three differential equations governing the slow change of amplitudes and phase difference

$$\begin{aligned} 2a_{1,\eta} &= a_1(1-\frac{a_1^2}{4}) + \kappa a_2 \sin\varphi, \\ 2a_{2,\eta} &= a_2(1-\frac{a_2^2}{4}) - \kappa a_1 \sin\varphi, \\ 2\varphi_{,\eta} &= \alpha + \kappa\cos\varphi\,(\frac{a_2}{a_1} - \frac{a_1}{a_2}). \end{aligned} \tag{7.33}$$

After finding the amplitudes and phase difference from (7.33), we can find k_1 from the previous equation for ϕ_1 by setting $\phi_1 = 0$. This is possible since the original system is autonomous.

The Slow Flow. Let us seek fixed points of the slow flow (7.33) representing synchronized vibrations of the coupled oscillators. We multiply the first equation of (7.33) (with the zero left-hand side) by a_1 and the second by a_2 and add together to get

$$a_1^2 + a_2^2 - \frac{a_1^4 + a_2^4}{4} = 0. \tag{7.34}$$

Next, multiplying the first equation of (7.33) by a_2 and the second by a_1 and subtracting them to obtain

$$\sin\varphi = \frac{a_1 a_2 (a_1^2 - a_2^2)}{4\kappa(a_1^2 + a_2^2)}.$$

From the third equation of (7.33) with $\varphi_{,\eta} = 0$ on the left-hand side follows

$$\cos\varphi = \frac{\alpha a_1 a_2}{\kappa(a_1^2 - a_2^2)}.$$

Using the identity $\sin^2 + \cos^2 = 1$ and setting

$$p = a_1^2 + a_2^2, \quad q = a_1^2 - a_2^2,$$

we get from the two last equations

$$q^6 - p^2 q^4 + (16\alpha^2 + 64\kappa^2) p^2 q^2 - 16\alpha^2 p^4 = 0.$$

In terms of p, q, equation (7.34) becomes

$$q^2 = 8p - p^2.$$

Substituting this equation into the previous one, we obtain finally

$$p^3 - 20p^2 + (16\alpha^2 + 32\kappa^2 + 128)p - (64\alpha^2 + 256\kappa^2 + 256) = 0. \tag{7.35}$$

This cubic equation has either 1 or 3 positive roots for p. At bifurcation, there will be a double root which appears if the derivative of (7.35) vanishes

$$3p^2 - 40p + 16\alpha^2 + 32\kappa^2 + 128 = 0. \tag{7.36}$$

Eliminating p from (7.35) and (7.36) gives the condition for saddle-node bifurcations as

$$\alpha^6 + (6\kappa^2 + 2)\alpha^4 + (12\kappa^4 - 10\kappa^2 + 1)\alpha^2 + 8\kappa^6 - \kappa^4 = 0. \tag{7.37}$$

Equation (7.37) plots as two curves intersecting as a cusp in the (α, κ)-plane (see Fig. 7.14). At the cusp, a further degeneracy occurs and there is a triple root of equation (7.35). Requiring the derivative of (7.36) to vanish yields $p = 20/3$ at the cusp, which gives the location of the cusp as

$$\alpha = \frac{1}{\sqrt{27}} \approx 0.1924, \quad \kappa = \frac{2}{\sqrt{27}} \approx 0.3849.$$

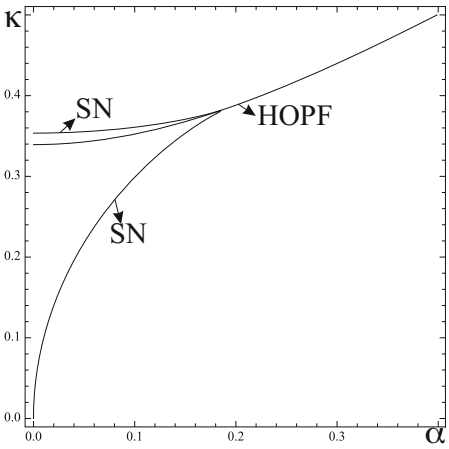

Fig. 7.14 Saddle-node and Hopf's bifurcation of coupled van der Pol's oscillator

Next, we look for Hopf's bifurcations of the slow flow (7.33). The presence of a stable limit cycle surrounding an unstable fixed point, as occurs in a supercritical Hopf's bifurcation, means a weakly locked quasiperiodic motion of the original system (7.30). Let $(a_{10}, a_{20}, \varphi_0)$ be a fixed point. The behavior of the system (7.33) linearized in the neighborhood of this point is determined by the eigenvalues of the Jacobian matrix

$$\frac{1}{2}\begin{pmatrix} -\frac{3a_{10}^2-4}{4} & \kappa\sin\varphi_0 & \kappa\cos\varphi_0 a_{20} \\ -\kappa\sin\varphi_0 & -\frac{3a_{20}^2-4}{4} & -\kappa\cos\varphi_0 a_{10} \\ -\frac{\kappa\cos\varphi_0(a_{10}^2+a_{20}^2)}{a_{10}^2 a_{20}} & \frac{\kappa\cos\varphi_0(a_{10}^2+a_{20}^2)}{a_{10}a_{20}^2} & -\frac{\kappa\sin\varphi_0(a_{20}^2-a_{10}^2)}{a_{10}a_{20}} \end{pmatrix}.$$

Using the above relations between a_1, a_2, $\sin\varphi$, $\cos\varphi$ and p, q, we can express the elements of this matrix in terms of p. The eigenvalues of this matrix are the roots of the cubic equation

$$\lambda^3 + c_2\lambda^2 + c_1\lambda + c_0 = 0,$$

where

$$\begin{aligned} c_2 &= \frac{p-4}{2}, \\ c_1 &= \frac{7p^3 - 112p^2 + (-16\alpha^2 + 512)p - 512}{64p - 512}, \\ c_0 &= \frac{p^4 - 22p^3 + 160p^2 - (32\alpha^2 + 384)p}{128p - 1024}. \end{aligned}$$

For a Hopf bifurcation to occur, the eigenvalues λ must include a pair of imaginary roots, $\pm i\beta$, and a real eigenvalue, γ. This requires the characteristic equation to have the form

$$\lambda^3 - \gamma\lambda^2 + \beta^2\lambda - \beta^2\gamma = 0.$$

Comparing these cubic equations, we see that a necessary condition for Hopf's bifurcation to occur is

$$c_0 = c_1c_2 \Rightarrow 3p^4 - 59p^3 + (-8\alpha^2 + 400)p^2 + (48\alpha^2 - 1088)p + 1024 = 0.$$

Eliminating p between this equation and (7.35) yields the condition for Hopf's bifurcation as

$$\begin{aligned} &49\alpha^8 + (266\kappa^2 + 238)\alpha^6 + (88\kappa^4 + 758\kappa^2 + 345)\alpha^4 + (-1056\kappa^6 \\ &+ 1099\kappa^4 + 892\kappa^2 + 172)\alpha^2 - 1152\kappa^8 - 2740\kappa^6 - 876\kappa^4 + 16 = 0. \end{aligned}$$

This equation plots as a curve in the (α, κ)-plane, which intersect the lower curve of saddle node bifurcation at point P and touches the upper curve of saddle-node bifurcation at point Q with the coordinates (see Fig. 7.15)

$$\text{P: } \alpha \approx 0.1918,\ \kappa \approx 0.3846, \quad \text{Q: } \alpha \approx 0.1899,\ \kappa \approx 0.3837.$$

We see that the main features of saddle-node and Hopf's bifurcations of a coupled van der Pol's oscillator are quite similar to those of forced van der Pol's oscillator discussed in Section 6.3. Strong synchronization occurs everywhere in the first quadrant of the (α, κ)-plane except in that region bounded by i) the lower curve of saddle node bifurcations from the origin to point P, ii) the curve of Hopf bifurcation from point P to infinity, and iii) the α-axis. However, there is an additional bifurcation here which did not occur in the forced problem. There is a homoclinic bifurcation which occurs along a curve emanating from point Q. This involves the destruction of the limit cycle which was born in the Hopf bifurcation. The limit cycle grows in size until it gets so large that it hits a saddle, and disappears in a saddle connection (see the details and further references in [10, 43]).

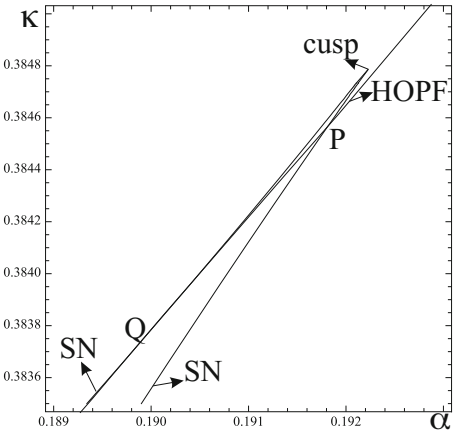

Fig. 7.15 Blowup of cusp region

In summary, we see that the transition from strongly synchronized vibrations to drifted vibrations involves an intermediate state in which the system is weakly synchronized. In the three-dimensional slow flow space, we go from a stable fixed point (strongly locked), to a stable limit cycle (weakly locked), and finally to a periodic motion which is topologically distinct from the original limit cycle (unlocked). As in the case of forced van der Pol's oscillator, in order for the strong synchronization to occur, we need either a small difference in uncoupled frequencies (small α) or a strong interaction of oscillators guaranteed by a large coupling factor κ.

7.5 Exercises

EXERCISE 7.1. Derive the equations of nonlinear vibration of the double pendulum considered in exercise 2.1.

Solution. Let us find the exact formula for the kinetic energy of the point-mass m_2. As seen from Fig. 2.14, the cartesian coordinates of this point-mass are

$$x_2 = l_1 \cos\varphi_1 + l_2 \cos\varphi_2, \quad y_2 = l_1 \sin\varphi_1 + l_2 \sin\varphi_2.$$

Thus, the kinetic energy of m_2 equals

$$K_2 = \frac{1}{2} m_2 (\dot{x}_2^2 + \dot{y}_2^2) = \frac{1}{2} m_2 [l_1^2 \dot{\varphi}_1^2 + l_2^2 \dot{\varphi}_2^2 + 2 l_1 l_2 \cos(\varphi_1 - \varphi_2) \dot{\varphi}_1 \dot{\varphi}_2].$$

Taking the kinetic energy of m_1 and the potential energy of the point-masses as in the solution of the exercise 2.1, we obtain the exact Lagrange function in the form

$$L = \frac{1}{2}(m_1+m_2)l_1^2\dot{\varphi}_1^2 + \frac{1}{2}m_2 l_2^2\dot{\varphi}_2^2 + m_2 l_1 l_2 \cos(\varphi_1-\varphi_2)\dot{\varphi}_1\dot{\varphi}_2 + (m_1+m_2)gl_1\cos\varphi_1 + m_2 g l_2 \cos\varphi_2.$$

After some simple transformations we obtain from Lagrange's equations

$$\ddot{\varphi}_1 + \alpha\cos(\varphi_1-\varphi_2)\ddot{\varphi}_2 + \alpha\sin(\varphi_1-\varphi_2)\dot{\varphi}_2^2 + \frac{g}{l_1}\sin\varphi_1 = 0,$$
$$\ddot{\varphi}_2 + \beta\cos(\varphi_1-\varphi_2)\ddot{\varphi}_1 - \beta\sin(\varphi_1-\varphi_2)\dot{\varphi}_1^2 + \frac{g}{l_2}\sin\varphi_2 = 0,$$

where

$$\alpha = \frac{m_2 l_2}{(m_1+m_2)l_1}, \quad \beta = \frac{l_1}{l_2}.$$

EXERCISE 7.2. Hamilton-Jacobi equation. Let the action function $S(q,t)$ be defined as the integral

$$S_{q_0,t_0}(q,t) = \int_\gamma L\,dt$$

along the extremal γ connecting the points (q_0,t_0) and (q,t). Show that $S(q,t)$ satisfies the Hamilton-Jacobi equation

$$\frac{\partial S}{\partial t} + H(q,\frac{\partial S}{\partial q}) = 0.$$

Solution. Let us first fix the time instant t and consider different extremals ending at different points q. Calculating the variation of S we get

$$\delta S = \frac{\partial L}{\partial \dot{q}}\cdot\delta q\Big|_{t_0}^{t} + \int_{t_0}^{t}\left(\frac{\partial L}{\partial q} - \frac{d}{dt}\frac{\partial L}{\partial \dot{q}}\right)\cdot\delta q\,dt = 0.$$

The second term vanishes because the variation is taken along the extremals satisfying Lagrange's equations. The first term, evaluated at the lower limit t_0 is also zero because q_0 is fixed. Replacing $\partial L/\partial\dot{q}$ by p, we obtain

$$\delta S = p\cdot\delta q,$$

and, consequently

$$\frac{\partial S}{\partial q} = p.$$

Now we let also t change. Then, it follows from the definition of S that its total time derivative equals L

$$\frac{dS}{dt} = L.$$

Using the chain rule of differentiation we have

$$\frac{dS}{dt} = \frac{\partial S}{\partial t} + \frac{\partial S}{\partial q}\cdot\dot{q} = \frac{\partial S}{\partial t} + p\cdot\dot{q}.$$

Thus,

$$\frac{\partial S}{\partial t} = L - p \cdot \dot{q} = -H(q,p).$$

Substituting $p = \partial S/\partial q$ into the Hamilton function and bringing $-H$ to the left-hand side, we obtain the Hamilton-Jacobi equation.

EXERCISE 7.3. Find the action variable for the Duffing oscillator with

$$H(q,p) = \frac{1}{2}(p^2 + U(q)), \quad U = U(q) = \frac{1}{2}q^2 + \frac{1}{4}\alpha q^4.$$

Solution. According to the definition of the action variable

$$I = \frac{1}{2\pi} \oint p dq.$$

We use the exact solution (5.12) of the Duffing equation to evaluate the contour integral. Since $p = \dot{q}$ and $dq = \dot{q}dt$ and since the phase curve is symmetric about the q- and $\dot{q}$-axes we have

$$\oint p dq = 4 \int_0^{q_M} p dq = 4 \int_0^{T/4} \dot{q}^2 dt.$$

Now we substitute the solution (5.12) into this integral. Since

$$q(t) = a\,\mathrm{cn}(bt,m), \quad \dot{q} = -ab\,\mathrm{sn}(bt,m)\mathrm{dn}(bt,m),$$

where

$$b = \sqrt{1+\alpha a^2}, \quad m = \frac{\alpha a^2}{2(1+\alpha a^2)},$$

the integral becomes

$$\oint p dq = 4 \int_0^{T/4} \dot{q}^2 dt = 4a^2b^2 \int_0^{T/4} \mathrm{sn}^2(bt,m)\mathrm{dn}^2(bt,m) dt.$$

Changing the variable t to $u = bt$ and taking into account that $bT/4 = K(m)$, we get

$$\oint p dq = 4a^2 b \int_0^{K(m)} \mathrm{sn}^2(u,m)\mathrm{dn}^2(u,m) du.$$

This integral of Jacobian elliptic functions can be computed analytically.[10] The result is

$$\oint p dq = 4a^2 b \frac{(-1+2m)E(m) + (1-m)K(m)}{3m},$$

where $K(m)$ and $E(m)$ are the complete elliptic integrals of the first and second kind, respectively. Thus, the action variable equals

[10] Use the formulas given in 5.13 of [3] or the symbolic integration with *Mathematica*.

$$I = \frac{2a^2 b}{\pi} \frac{(-1+2m)E(m) + (1-m)K(m)}{3m}.$$

The total energy of the Duffing oscillator depends on the amplitude a as follows

$$H = \frac{1}{2}a^2 + \frac{1}{4}\alpha a^4.$$

Using the properties of the complete elliptic integrals one can show that

$$\frac{dI}{da} = \frac{2abK(m)}{\pi}.$$

Therefore

$$\frac{dH}{dI} = \frac{dH/da}{dI/da} = \frac{a(1+a^2)\pi}{2abK(m)} = \frac{\pi b}{2K(m)} = \frac{2\pi}{T} = \omega(a).$$

EXERCISE 7.4. Simulate numerically the Poincaré map for the Hénon-Heiles equations which can be obtained as Lagrange's equation of the following Lagrange function

$$L = \frac{1}{2}(\dot{x}^2 + \dot{y}^2) - \frac{1}{2}(x^2 + y^2 + 2x^2 y - \frac{2}{3}y^3).$$

Choose the cut plane $x = 0$ and the total energy i) $E_0 = 0.01$ and ii) $E_0 = 1/8$. Observe the difference in cases i) and ii).

Solution. Let us derive the equations of motion of these coupled oscillators in the Hamilton's form. Denoting $q_1 = x$, $q_2 = y$ and introducing $p_1 = \dot{q}_1$, $\dot{p}_2 = \dot{q}_2$, we transform the above Lagrange function to the Hamilton function

$$H = \frac{1}{2}(p_1^2 + p_2^2) + \frac{1}{2}(q_1^2 + q_2^2 + 2q_1^2 q_2 - \frac{2}{3}q_2^3).$$

Hamilton's equations are

$$\dot{q}_1 = p_1, \quad \dot{p}_1 = -(q_1 + 2q_1 q_2),$$
$$\dot{q}_2 = p_2, \quad \dot{p}_2 = -(q_2 - q_2^2 + q_1^2).$$

This dynamical system has one stable fixed point at the origin $(0,0)$ and three unstable fixed points given by

$$\mathrm{P}_1 : (0,1), \quad \mathrm{P}_2 : (\sqrt{3}/2, -1/2), \quad \mathrm{P}_3 : (-\sqrt{3}/2, -1/2).$$

The contour plot of the potential energy $U(q) = \frac{1}{2}(q_1^2 + q_2^2 + 2q_1^2 q_2 - \frac{2}{3}q_2^3)$ is shown in Fig. 7.16. The separatrices connecting the unstable fixed points are straight lines and correspond to the energy level $1/6$. All contours with the potential energies less than $1/6$ are inside the triangle $\mathrm{P}_1\mathrm{P}_2\mathrm{P}_3$.

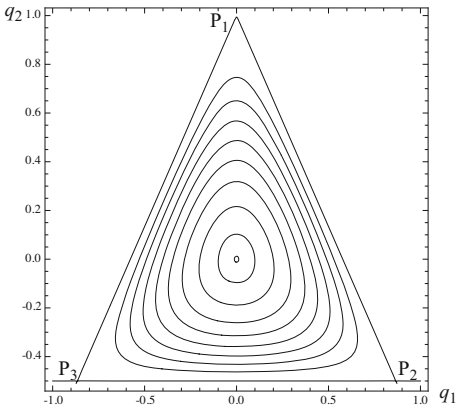

Fig. 7.16 Contour plot of the potential energy of Henon-Heiles oscillators

As the dynamical system of Henon-Heiles oscillators is conservative, the energy conservation reads

$$H(q,p) = E_0,$$

and the phase curves having the initial energy E_0 must lie on some 3-D energy level surface. We use this integral to find p_1. Then the phase curves must be found in some 3-D space of parameters q_1, q_2, p_2. To follow the traces of these phase curves we choose the cut plane $q_1 = 0$ and plot the Poincaré map numerically using the code written by Weinstein. The results are shown in Fig. 7.17 for the case $E_0 = 10^{-2}$ (left) and $E_0 = 1/8$ (right), respectively. For $E_0 = 10^{-2}$ we see four families of embedded tories corresponding to ordered motion. For $E_0 = 1/8$ one observes a chaotic see surrounding small islands of ordered motion.

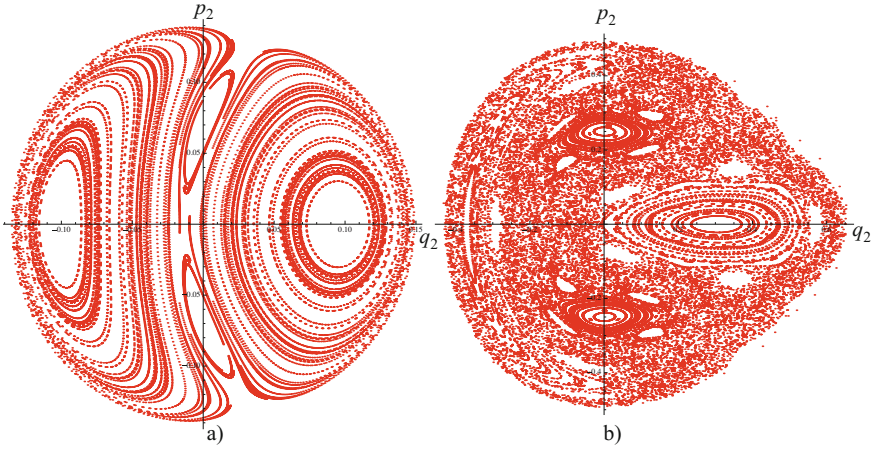

Fig. 7.17 Poincaré maps of Henon-Heiles oscillators: a) $E_0 = 0.01$, b) $E_0 = 1/8$

EXERCISE 7.5. Modal equation in a rotating frame. In the frame rotating with the constant angular velocity ω, the presence of Coriolis and centripetal accelerations changes the equations of motion (7.7) to

$$\ddot{x} - 2\omega\dot{y} - \omega^2 x = -\frac{\partial U}{\partial x}, \quad \ddot{y} + 2\omega\dot{x} - \omega^2 y = -\frac{\partial U}{\partial y}.$$

For this system, obtain a first integral and use it to derive a modal equation for the orbits in the (x,y)-plane which does not involve time t.

Solution. The first integral can easily be obtained if we know the kinetic and potential energies. The absolute velocity of the point-mass equals

$$\mathbf{v} = \mathbf{v}_l + \mathbf{v}_r,$$

where $\mathbf{v}_l = \omega \times \mathbf{r} = (-\omega y, \omega x)$ is the instantaneous velocity of the point-mass rotating together with the frame about the z-axis and $\mathbf{v}_r = (\dot{x}, \dot{y})$ the relative velocity. Thus,

$$\mathbf{v} = (\dot{x} - \omega y, \dot{y} + \omega x),$$

and the kinetic energy for $m = 1$ becomes

$$K = \frac{1}{2}[(\dot{x} - \omega y)^2 + (\dot{y} + \omega x)^2].$$

Together with the potential energy $U(x,y)$, the conservation of the total energy reads

$$\frac{1}{2}[(\dot{x} - \omega y)^2 + (\dot{y} + \omega x)^2] + U(x,y) = E_0.$$

We seek the nonlinear normal modes as periodic solutions by assuming y as a function of x, without direct reference to time t, and try to eliminate t in these equations. Using the chain rule

$$\dot{y} = y'\dot{x}, \quad \ddot{y} = y''\dot{x}^2 + y'\ddot{x},$$

with prime denoting the derivative of y with respect to x, and substituting this into the Lagrange equation for y to get

$$-\frac{\partial U}{\partial y} = y''\dot{x}^2 + y'(2\omega y'\dot{x} + \omega^2 x - \frac{\partial U}{\partial x}) - 2\omega\dot{x} - \omega^2 y.$$

Next, we plug $\dot{y}$ into the energy conservation

$$\frac{1}{2}[\dot{x}^2(1 + y'^2) + 2\omega(xy' - y)\dot{x} + \omega^2(x^2 + y^2)] + U(x,y) = E_0.$$

Solving this equation with respect to $\dot{x}$, we obtain

$$\dot{x} = \frac{-\omega(xy' - y) \pm \sqrt{\omega^2(xy' - y)^2 - (1 + y'^2)[\omega^2(x^2 + y^2) + 2U(x,y) - 2E_0]}}{1 + y'^2}.$$

Substituting this formula into the above equation, we derive the nonlinear modal equation in terms of $y(x)$.

EXERCISE 7.6. A rigid bar, connected with two linear springs of stiffnesses k_1 and k_2, carries out a translational motion of its center of mass S in the vertical direction and a rotation in the plane about S (see Fig. 7.18). The supports A and B can freely move in the horizontal direction to keep the springs in the vertical position. Derive the equations of motion for finite x and φ. Obtain a first integral and use it to derive a modal equation.

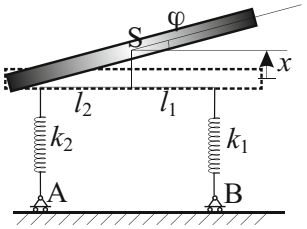

Fig. 7.18 Nonlinear model of vehicle

Solution. Let $q = (x, \varphi)$ denote the generalized coordinates. We write down the kinetic and potential energies of this system as follows

$$\begin{aligned} K(\dot{q}) &= \frac{1}{2}m\dot{x}^2 + \frac{1}{2}J_S\dot{\varphi}^2, \\ U(q) &= \frac{1}{2}k_1(x_{st} + x + l_1\sin\varphi)^2 + \frac{1}{2}k_2(x_{st} + x - l_2\sin\varphi)^2 + mgx \\ &= \frac{1}{2}k_1(x + l_1\sin\varphi)^2 + \frac{1}{2}k_2(x - l_2\sin\varphi)^2 \\ &\quad + ((k_1 + k_2)x_{st} + mg)x + (k_1l_1 - k_2l_2)\sin\varphi + \frac{1}{2}(k_1 + k_2)x_{st}^2. \end{aligned}$$

Taking the force and moment equilibrium

$$(k_1 + k_2)x_{st} + mg = 0, \quad (k_1l_1 - k_2l_2)x_{st} = 0$$

into account and removing the last constant term in the potential energy, we can represent it in the form

$$U(x, \varphi) = \frac{1}{2}k_1(x + l_1\sin\varphi)^2 + \frac{1}{2}k_2(x - l_2\sin\varphi)^2.$$

It is now straightforward to derive Lagrange's equations

$$\begin{aligned} m\ddot{x} + (k_1 + k_2)x + (k_1l_1 - k_2l_2)\sin\varphi &= 0, \\ J_S\ddot{\varphi} + (k_1l_1 - k_2l_2)x\cos\varphi + \frac{1}{2}(k_1l_1^2 + k_2l_2^2)\sin 2\varphi &= 0. \end{aligned}$$

The first integral corresponding to the energy conservation follows

$$\frac{1}{2}m\dot{x}^2+\frac{1}{2}J_S\dot{\varphi}^2+U(x,\varphi)=E_0.$$

On the other hand, we can represent the equations of motion in the short form

$$m\ddot{x}=-\frac{\partial U}{\partial x},\quad J_S\ddot{\varphi}=-\frac{\partial U}{\partial \varphi}.$$

To derive the modal equation, we assume φ as a function of x, without direct reference to time t, and try to eliminate t in these equations. That is, we assume $\varphi=\varphi(x)$ and compute its time derivatives according to the chain rule

$$\dot{\varphi}=\varphi'(x)\dot{x},\quad \ddot{\varphi}=\varphi''(x)\dot{x}^2+\varphi'(x)\ddot{x},$$

with prime denoting the derivative of φ with respect to x. Using the first equation of motion to compute the acceleration $\ddot{x}$ and substituting it into the second equation, we get

$$J_S[\varphi''(x)\dot{x}^2-\frac{1}{m}\varphi'(x)\frac{\partial U}{\partial x}]=-\frac{\partial U}{\partial \varphi}.$$

Next, we substitute $\dot{\varphi}$ into the energy conservation and solve the latter with respect to $\dot{x}$ to find

$$\dot{x}^2=\frac{2[E_0-U(x,\varphi)]}{m+J_S\varphi'(x)^2}.$$

The modal equation can finally be obtained by substituting this expression into the above equation

$$J_S\left\{\varphi''(x)\frac{2[E_0-U(x,\varphi)]}{m+J_S\varphi'(x)^2}-\frac{1}{m}\varphi'(x)\frac{\partial U}{\partial x}\right\}=-\frac{\partial U}{\partial \varphi}.$$

This last equation can be transformed to

$$2[E_0-U(x,\varphi)]\varphi''(x)+[m+J_S\varphi'(x)^2][\frac{1}{J_S}\frac{\partial U}{\partial \varphi}-\frac{1}{m}\varphi'(x)\frac{\partial U}{\partial x}]=0,$$

where

$$\frac{\partial U}{\partial x}=(k_1+k_2)x+(k_1l_1-k_2l_2)\sin\varphi,$$
$$\frac{\partial U}{\partial \varphi}=(k_1l_1-k_2l_2)x\cos\varphi+\frac{1}{2}(k_1l_1^2+k_2l_2^2)\sin 2\varphi.$$

EXERCISE 7.7. Derive equations (7.14).

Solution. We shall derive this system of equations from the equations of slow flow for A_1, B_1, A_2, B_2 obtained in Section 7.2 by the variational asymptotic method

$$A_{1,\eta} = \frac{3}{8}B_1(A_1^2+B_1^2) + \frac{3}{8}B_1(A_2^2+B_2^2) + \frac{3}{4}B_2(A_1A_2+B_1B_2),$$
$$B_{1,\eta} = -\frac{3}{8}A_1(A_1^2+B_1^2) - \frac{3}{8}A_1(A_2^2+B_2^2) - \frac{3}{4}A_2(A_1A_2+B_1B_2),$$
$$A_{2,\eta} = (\frac{3}{8}+3\kappa)B_2(A_2^2+B_2^2) + \frac{3}{8}B_2(A_1^2+B_1^2) + \frac{3}{4}B_1(A_1A_2+B_1B_2),$$
$$B_{2,\eta} = -(\frac{3}{8}+3\kappa)A_2(A_2^2+B_2^2) - \frac{3}{8}A_2(A_1^2+B_1^2) - \frac{3}{4}A_1(A_1A_2+B_1B_2).$$

Multiplying the first equation by A_1, the second by B_1, and adding them together, we obtain

$$A_1A_{1,\eta} + B_1B_{1,\eta} = \frac{3}{4}(A_1A_2+B_1B_2)(A_1B_2-A_2B_1).$$

Using the definitions of the amplitudes and the phase difference, it is easy to see that the following identities

$$A_1A_{1,\eta} + B_1B_{1,\eta} = \frac{1}{2}\frac{d}{d\eta}(A_1^2+B_1^2) = \frac{1}{2}\frac{d}{d\eta}a_1^2,$$
$$A_1A_2 + B_1B_2 = a_1a_2\cos(\phi_2-\phi_1) = a_1a_2\cos\varphi,$$
$$A_1B_2 - A_2B_1 = a_1a_2\sin(\phi_2-\phi_1) = a_1a_2\sin\varphi$$

hold true transforming the above equation to

$$a_1a_{1,\eta} = \frac{3}{8}a_1^2a_2^2\sin 2\varphi \quad \Rightarrow \quad a_{1,\eta} = \frac{3}{8}a_1a_2^2\sin 2\varphi.$$

Thus, the first equation has been proved. The second equation for a_2 can be derived similarly. In this case we multiply the third and the fourth equations of the above system by A_2 and B_2, respectively, and then add them together. The result is

$$\frac{1}{2}\frac{d}{d\eta}(A_2^2+B_2^2) = \frac{3}{4}(A_2B_1-A_1B_2)(A_1A_2+B_1B_2).$$

With supplement of the following identity

$$A_2B_1 - A_1B_2 = -a_1a_2\sin\varphi,$$

we transform this equation to

$$a_2a_{2,\eta} = -\frac{3}{8}a_1^2a_2^2\sin 2\varphi \quad \Rightarrow \quad a_{2,\eta} = -\frac{3}{8}a_1^2a_2\sin 2\varphi.$$

To derive the equation for the phase difference, we multiply the first equation by A_2, the second by B_2, the third by A_1, and the last by B_1, and then add them together. The latter, after some calculation, can be written as

$$\frac{d}{d\eta}(A_1A_2+B_1B_2)=3\kappa(A_1B_2-A_2B_1)(A_2^2+B_2^2).$$

The derivative on the left-hand side of this equation can be expressed in terms of a_1, a_2 and φ according to

$$\begin{aligned}\frac{d}{d\eta}(a_1a_2\cos\varphi) &= (a_{1,\eta}a_2+a_1a_{2,\eta})\cos\varphi - a_1a_2\varphi_{,\eta}\sin\varphi\\ &= (\frac{3}{8}a_1a_2^3\sin 2\varphi-\frac{3}{8}a_1^3a_2\sin 2\varphi)\cos\varphi - a_1a_2\varphi_{,\eta}\sin\varphi\\ &= [\frac{3}{4}a_1a_2(a_2^2-a_1^2)\cos^2\varphi - a_1a_2\varphi_{,\eta}]\sin\varphi,\end{aligned}$$

whereas the right-hand side is simply $3\kappa a_1a_2^3\sin\varphi$. Plugging these into the above equation and dividing both sides by $a_1a_2\sin\varphi$, we obtain the evolution equation for the phase difference

$$\varphi_{,\eta}=\frac{3}{4}(a_2^2-a_1^2)\cos^2\varphi-3\kappa a_2^2,$$

which, by recalling $\cos^2\varphi=(1+\cos 2\varphi)/2$, can be rewritten as

$$\varphi_{,\eta}=-\frac{3}{8}(a_1^2+a_2^2)+3(\frac{1}{4}-\kappa)a_2^2+\frac{3}{8}(a_2^2-a_1^2)\cos 2\varphi.$$

EXERCISE 7.8. Compute the approximate Poincaré map from the first integral (7.17) numerically for the energy level $E_0=0.4$ and for the parameter $\varepsilon=0.1$, $\kappa=0.1$, and compare it with the Poincaré map obtained by the numerical integration of the exact equations (7.1).

Solution. In order to compute the Poincaré map of the exact equations (7.1) we adapt the *Mathematica* code written by Weisstein to them. Such modified code is shown below. There are two main functions: the first is used to produce surface of section by condition $x=0$ with the given initial conditions $x(0)=x_0$, $y(0)=y_0$ and $\dot{y}(0)=\dot{y}_0$, whereas the second plots the result using the ListPlot command. The initial velocity $\dot{x}(0)$ should be computed through others by using the first integral

$$\frac{1}{2}\dot{x}^2+\frac{1}{2}\dot{y}^2+\frac{1}{2}(x^2+y^2)+\frac{\alpha}{4}(x^4+y^4)+\frac{\beta}{4}(y-x)^4=E_0,$$

which implies

$$\dot{x}_0=\sqrt{2E_0-\dot{y}_0^2-(x_0^2+y_0^2)-\frac{\alpha}{2}(x_0^4+y_0^4)-\frac{\beta}{2}(y_0-x_0)^4}.$$

```
SurfaceOfSection[{x0_, {y0_, dy0_}, e_, α_, β_}, tmax_] :=
 Module[{dx0 = Sqrt[2 e - x0^2 - y0^2 - α/2 x0^4 - α/2 y0^4 - β/2 (y0 - x0)^4 - dy0^2]}, x, y, t},
  If[# == {}, {}, First[#]] &@Last[Reap[NDSolve[{
       x''[t] == -x[t] - α x[t]^3 + β (y[t] - x[t])^3,
       y''[t] == -y[t] - α y[t]^3 - β (y[t] - x[t])^3,
       y[0] == y0, y'[0] == dy0, x[0] == x0, x'[0] == dx0},
      {x, y}, {t, 0, tmax}, Method → {EventLocator, "Event" → x[t],
        "EventCondition" → (x'[t] > 0.), "EventAction" :↦ Sow[{y[t], y'[t]}]}
     ]]]
 ]
Internal`DeactivateMessages[ListPlot[
  SurfaceOfSection[{0., {0., -0.65}, 0.4, 0.1, 0.01}, 2000],
  PlotStyle → {PointSize[.005], Black},
  AspectRatio → Automatic, AxesLabel -> TraditionalForm /@ {y[t], ẏ[t] },
  ImageSize → 500]]
```

The map obtained from the first integral (7.17) can be plotted with the ParametricPlot command. The comparison of these two maps was shown in Fig. 7.11.

EXERCISE 7.9. Prove the formulas $(7.29)_{2,3}$.

Solution. Let us recall the definitions of matrices A, B, and C

$$A = U^T L_{,vv} U, \quad B = U^T L_{,v\varphi} - L^T_{,v\varphi} U, \quad C = U^T E_{,\varphi},$$

where the following abbreviations are used

$$L_{,v\varphi} = \frac{\partial}{\partial \varphi} L_{,v}(u(\varphi), \nabla u(\varphi)), \quad E_{,\varphi} = \frac{\partial}{\partial \varphi} E(L,u), \quad U = \frac{\partial u}{\partial \varphi}.$$

Consider first the matrix B with the elements

$$B_{ij} = U^T_{im}[L_{,v\varphi}]_{mj} - [L^T_{,v\varphi}]_{im} U_{mj},$$

where the elements of matrices U and $L_{,v\varphi}$ are given by

$$U_{im} = \frac{\partial u_i}{\partial \varphi_m}, \quad [L_{,v\varphi}]_{mj} = \frac{\partial}{\partial \varphi_j} \frac{\partial L}{\partial v_m}.$$

Using these formulas for U and $L_{,v\varphi}$, we compute B_{ij} explicitly

$$\begin{aligned} B_{ij} &= \frac{\partial u_m}{\partial \varphi_i} \frac{\partial}{\partial \varphi_j} \frac{\partial L}{\partial v_m} - \frac{\partial}{\partial \varphi_i} \frac{\partial L}{\partial v_m} \frac{\partial u_m}{\partial \varphi_j} \\ &= \frac{\partial}{\partial \varphi_i}(u_m \frac{\partial}{\partial \varphi_j} \frac{\partial L}{\partial v_m}) - u_m \frac{\partial^2}{\partial \varphi_i \partial \varphi_j} \frac{\partial L}{\partial v_m} \\ &- \frac{\partial}{\partial \varphi_j}(u_m \frac{\partial}{\partial \varphi_i} \frac{\partial L}{\partial v_m}) + u_m \frac{\partial^2}{\partial \varphi_j \partial \varphi_i} \frac{\partial L}{\partial v_m} \\ &= \frac{\partial}{\partial \varphi_i}(u_m \frac{\partial}{\partial \varphi_j} \frac{\partial L}{\partial v_m}) - \frac{\partial}{\partial \varphi_j}(u_m \frac{\partial}{\varphi_i} \frac{\partial L}{\partial v_m}), \end{aligned}$$

where the identity of mixed derivatives

$$\frac{\partial^2}{\partial\varphi_i\partial\varphi_j}(\cdot)=\frac{\partial^2}{\partial\varphi_j\partial\varphi_i}(\cdot)$$

has been taken into account. Since u_m and v_m are 2π-periodic in each variable φ_k, so are the expressions in the above parentheses. Thus, it follows immediately that

$$\int_{T^n}B_{ij}=0.$$

Next, we turn to the vector $Q=U^TE(L,u)$, whose components are

$$\begin{aligned}Q_i=U_{ik}^TE_k(L,u)&=\frac{\partial u_k}{\partial\varphi_i}(\nabla\frac{\partial L}{\partial\dot{q}_k}(u,\nabla u)-\frac{\partial}{\partial q_k}L(u,\nabla u))\\&=\frac{\partial u_k}{\partial\varphi_i}\omega_j\frac{\partial}{\partial\varphi_j}\frac{\partial L}{\partial v_k}(u,\nabla u)-\frac{\partial u_k}{\partial\varphi_i}\frac{\partial L}{\partial u_k}(u,\nabla u)\\&=\omega_j\frac{\partial}{\partial\varphi_j}[\frac{\partial L}{\partial v_k}(u,\nabla u)\frac{\partial u_k}{\partial\varphi_i}]-\frac{\partial L}{\partial v_k}(u,\nabla u)\omega_j\frac{\partial^2u_k}{\partial\varphi_j\partial\varphi_i}-\frac{\partial u_k}{\partial\varphi_i}\frac{\partial L}{\partial u_k}(u,\nabla u).\end{aligned}$$

Noticing that

$$\omega_j\frac{\partial^2u_k}{\partial\varphi_j\partial\varphi_i}=\frac{\partial}{\partial\varphi_i}\frac{\partial u_k}{\partial\varphi_j}\frac{d\varphi_j}{dt}=\frac{\partial v_k}{\partial\varphi_i},$$

the expression for Q_i reduces to

$$Q_i=\omega_j\frac{\partial}{\partial\varphi_j}[\frac{\partial L}{\partial v_k}(u,\nabla u)\frac{\partial u_k}{\varphi_i}]-\frac{\partial L}{\partial\varphi_i}.$$

Using the periodicity condition of u and v with respect to φ, we see that the integral of Q_i on the torus also vanishes

$$\int_{T^n}U_{ik}^TE_k(L,u)=0.$$

EXERCISE 7.10. Simulate numerically the solutions of equations (7.30) satisfying the initial conditions $x(0)=1$, $\dot{x}(0)=0$ and $y(0)=1$, $\dot{y}(0)=0$ for $\varepsilon=0.1$, $\alpha=1$, and $\kappa=1.2$. Plot the curves $x(t)$, $y(t)$, and $x(t)y(t)$ and compare them with the corresponding curves obtained from the slow flow system (7.33). Explain why synchronization leads to the stationary behavior of the amplitude modulation of $x(t)y(t)$.

Solution. In order to compare the numerical solutions $x(t)$, $y(t)$ of the exact equations (7.30) and their amplitude modulations obeying the slow flow equations (7.33), we need to refer (7.33) to the same time variable. Thus, it is necessary to solve the slow flow equations in $\tau=\omega t$ by changing from η to τ according to

$$\frac{d}{d\eta}(\cdot)=\frac{d}{d\tau}(\cdot)\frac{d\tau}{d\eta}=\frac{1}{\varepsilon}\frac{d}{d\tau}(\cdot).$$

The following pieces of code in *Mathematica* provide the numerical solutions to the systems (7.30) and (7.33). The curves $x(t)$ and $y(t)$ corresponding to the numerical solution of (7.30) as well as their amplitude modulations are shown in Fig. 7.19.

```
sol = NDSolve[{x''[t] + x[t] + ϵ κ (x[t] - y[t]) - ϵ (1 - x[t]^2) x'[t] == 0,
    y''[t] + (1 + ϵ α) y[t] - ϵ κ (x[t] - y[t]) - ϵ (1 - y[t]^2) y'[t] == 0,
    x[0] == 1, x'[0] == 0, y[0] == 1, y'[0] == 0}, {x[t], y[t]}, {t, 0, 5 × 10^2}];
slow = NDSolve[{2/ϵ a1'[t] == a1[t] (1 - a1[t]^2/4) + κ a2[t] Sin[φ[t]],
    2/ϵ a2'[t] == a2[t] (1 - a2[t]^2/4) - κ a1[t] Sin[φ[t]],
    2/ϵ φ'[t] == α + κ Cos[φ[t]] (a2[t]/a1[t] - a1[t]/a2[t]), a1[0] == 1, a2[0] == 1, φ[0] == 0},
  {a1[t], a2[t], φ[t]}, {t, 0, 500}];
```

Based on the variational-asymptotic analysis we can present the asymptotic solution (in the first approximation) to the equations of coupled oscillators in the form

$$x_0(t,\eta) = a_1(\eta)\cos(\omega t - \phi_1(\eta)), \quad y_0(t,\eta) = a_2(\eta)\cos(\omega t - \phi_2(\eta)),$$

where $\eta = \varepsilon\tau = \varepsilon\omega t$. Using the product rule of trigonometric functions, we compute their product

$$z_0(t,\eta) = x_0(t,\eta)y_0(t,\eta) = \frac{1}{2}a_1(\eta)a_2(\eta)[\cos(2\omega t - \phi_1(\eta) - \phi_2(\eta)) + \cos\varphi(\eta)].$$

In the expression in square brackets the first summand containing the fast variable t describes the fast oscillating contribution to the product with the amplitude $\frac{1}{2}a_1a_2$, while the second summand describes the slow oscillating contribution with the same amplitude. Thus, the amplitude modulation of $x(t)y(t)$ at large time can be described asymptotically as

$$a(\eta) = \frac{1}{2}a_1(\eta)a_2(\eta)(1 + \cos\varphi(\eta)).$$

We see that if strong synchronization occurs, then $a(\eta)$ must approach a constant value. The curve $x(t)y(t)$ corresponding to the numerical solution of (7.30) as well as its amplitude modulation, shown in Fig. 7.20, indicates the occurrence of strong synchronization and confirms the analysis provided in Section 7.4.

EXERCISE 7.11. Recheck the slow flow equations (7.33).

Solution. We recall the equations of slow flow for $A_j(\eta)$ and $B_j(\eta)$ obtained in Section 7.4

$$2A_{1,\eta} = -2k_1B_1 + A_1 - \frac{A_1}{4}(A_1^2 + B_1^2) + \kappa(B_1 - B_2),$$
$$2B_{1,\eta} = 2k_1A_1 + B_1 - \frac{B_1}{4}(A_1^2 + B_1^2) + \kappa(A_2 - A_1),$$

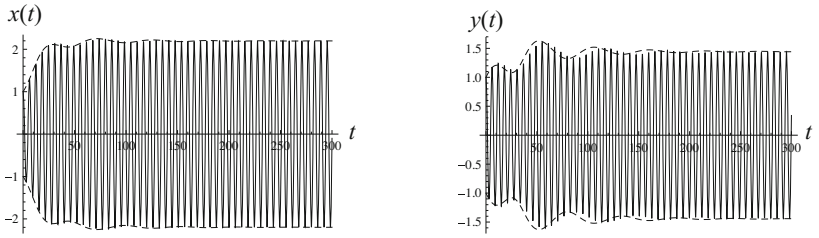

Fig. 7.19 Curves $x(t)$ and $y(t)$ corresponding to the numerical solution of (7.30) (bold lines) and their amplitude modulations in accordance with (7.33) (dashed lines)

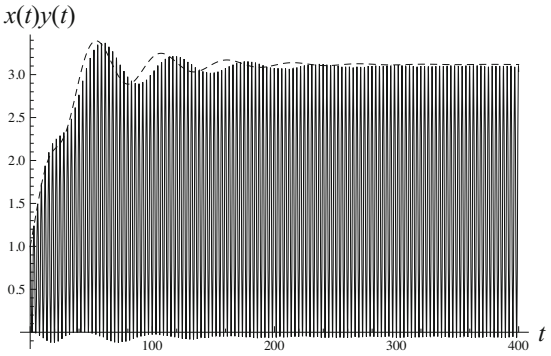

Fig. 7.20 Numerical simulation of the product $x(t)y(t)$ (bold line) and its amplitude modulation (dashed line)

$$2A_{2,\eta} = -2k_1B_2 + \alpha B_2 + A_2 - \frac{A_2}{4}(A_2^2 + B_2^2) + \kappa(B_2 - B_1),$$
$$2B_{2,\eta} = 2k_1A_2 - \alpha A_2 + B_2 - \frac{B_2}{4}(A_2^2 + B_2^2) + \kappa(A_1 - A_2).$$

Multiplying the first equation by A_1, the second by B_1, and adding them, then performing the similar operations for the third and the fourth equations, we obtain

$$2(A_1A_{1,\eta} + B_1B_{1,\eta}) = A_1^2 + B_1^2 - \frac{1}{4}(A_1^2 + B_1^2)^2 + \kappa(A_2B_1 - A_1B_2),$$
$$2(A_2A_{2,\eta} + B_2B_{2,\eta}) = A_2^2 + B_2^2 - \frac{1}{4}(A_2^2 + B_2^2)^2 - \kappa(A_2B_1 - A_1B_2).$$

Expressing A_j and B_j in terms of a_1, a_2 and ϕ_1, ϕ_2, this system can be rewritten as

$$2a_1a_{1,\eta} = a_1^2 - \frac{a_1^4}{4} + \kappa a_1a_2\sin(\phi_1 - \phi_2),$$
$$2a_2a_{2,\eta} = a_2^2 - \frac{a_2^4}{4} - \kappa a_1a_2\sin(\phi_1 - \phi_2),$$

which is equivalent to

$$2a_{1,\eta} = a_1(1-\frac{a_1^2}{4}) + \kappa a_2 \sin\varphi,$$
$$2a_{2,\eta} = a_2(1-\frac{a_2^2}{4}) - \kappa a_1 \sin\varphi,$$

where $\varphi = \phi_1 - \phi_2$ is the phase difference.

Returning to the system of slow flow equations, we rewrite them in terms of a_1, a_2, ϕ_1, ϕ_2 as follows

$$\begin{aligned}
2(a_{1,\eta}\cos\phi_1 - a_1\sin\phi_1\phi_{1,\eta}) &= -2k_1a_1\sin\phi_1 + a_1\cos\phi_1 \\
&\quad - \frac{1}{4}a_1^3\cos\phi_1 + \kappa(a_1\sin\phi_1 - a_2\sin\phi_2), \\
2(a_{1,\eta}\sin\phi_1 + a_1\cos\phi_1\phi_{1,\eta}) &= 2k_1a_1\cos\phi_1 + a_1\sin\phi_1 \\
&\quad - \frac{1}{4}a_1^3\sin\phi_1 + \kappa(a_2\cos\phi_2 - a_1\cos\phi_1), \\
2(a_{2,\eta}\cos\phi_2 - a_2\sin\phi_2\phi_{2,\eta}) &= -2k_1a_2\sin\phi_2 + \alpha a_2\sin\phi_2 + a_2\cos\phi_2 \\
&\quad - \frac{1}{4}a_2^3\cos\phi_2 + \kappa(a_2\sin\phi_2 - a_1\sin\phi_1), \\
2(a_{2,\eta}\sin\phi_2 + a_2\cos\phi_2\phi_{2,\eta}) &= 2k_1a_2\cos\phi_2 - \alpha a_2\cos\phi_2 + a_2\sin\phi_2 \\
&\quad - \frac{1}{4}a_2^3\sin\phi_2 + \kappa(a_1\cos\phi_1 - a_2\cos\phi_2).
\end{aligned}$$

Multiplying the first equation by $\sin\phi_1$, the second by $\cos\phi_1$, subtracting the first equation from the second one, and using the identity $\sin^2\phi + \cos^2\phi = 1$, we obtain

$$2\phi_{1,\eta} = 2k_1 - \kappa + \kappa\frac{a_2}{a_1}\cos(\phi_1 - \phi_2).$$

In a similar manner, we multiply the third equation by $\sin\phi_2$, the fourth by $\cos\phi_2$ and subtract one from another to get

$$2\phi_{2,\eta} = 2k_1 - \alpha - \kappa + \kappa\frac{a_1}{a_2}\cos(\phi_1 - \phi_2).$$

The evolution equation for the phase difference $\varphi = \phi_1 - \phi_2$ is easily derived by subtracting one from another of two equations just obtained yielding

$$2\varphi_{,\eta} = \alpha + (\frac{a_2}{a_1} - \frac{a_1}{a_2})\cos\varphi.$$

EXERCISE 7.12. Solve the slow flow system (7.33) numerically for $\alpha = 1$, and $\kappa = 1.2$, with the initial conditions $a_1(0) = 1$, $a_2(0) = 1$, and $\varphi(0) = 1$. Plot the curves $a_1(t)$, $a_2(t)$, and $\varphi(t)$, and observe their behavior as t becomes large.

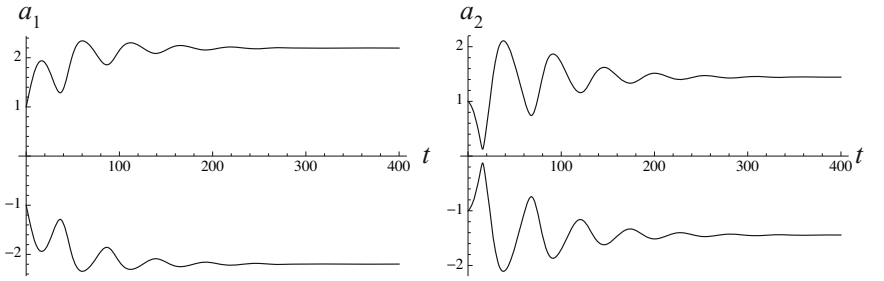

Fig. 7.21 Amplitudes $a_1(t)$ and $a_2(t)$ of the weakly coupled van der Pol's oscillators

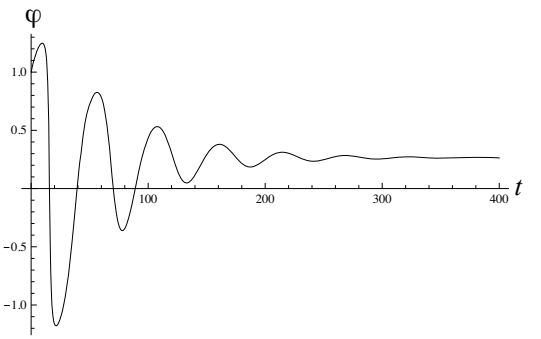

Fig. 7.22 The phase difference $\varphi(t)$ of the weakly coupled van der Pol's oscillators

Solution. The numerical solution of the system can be obtained via the NDSolve command provided in *Mathematica*. The plotted curves of amplitudes $a_1(t)$ and $a_2(t)$ are shown adjacent to each other in Fig. 7.21, where it can be seen that they stay constant as time t tends to infinity. The next Figure 7.22 shows the plot of the phase difference $\varphi(t)$. Observe that the phase difference also approaches a constant value as time goes to infinity. The figures illustrated here are generated using the numerical solution obtained with the following piece of code.

```
slow = NDSolve[{2/ϵ a1'[t] == a1[t] (1 - a1[t]^2/4) + κ a2[t] Sin[φ[t]],
    2/ϵ a2'[t] == a2[t] (1 - a2[t]^2/4) - κ a1[t] Sin[φ[t]],
    2/ϵ φ'[t] == α + κ Cos[φ[t]] (a2[t]/a1[t] - a1[t]/a2[t]), a1[0] == 1, a2[0] == 1, φ[0] == 0},
  {a1[t], a2[t], φ[t]}, {t, 0, 500}];
```

The behavior of the amplitudes and of the phase difference indicates that, after a short transient time of unsynchronized oscillations of the amplitudes, the steady-state synchronized vibrations of the coupled oscillators occur. This is also confirmed by the analysis of the coupled self-excited oscillators provided in Section 7.4 and by Fig. 7.14.